



UNIVERSIDADE
ESTADUAL DE LONDRINA

PAULO DA SILVA WATANABE

**ALTERAÇÕES MORFOLÓGICAS E FISIOLÓGICAS NO
CÓLON DE CAMUNDONGOS COM RETOCOLITE
ULCERATIVA AGUDA E CRÔNICA INDUZIDA POR
DEXTRAN SULFATO DE SÓDIO**

PAULO DA SILVA WATANABE

**ALTERAÇÕES MORFOLÓGICAS E FISIOLÓGICAS NO
CÓLON DE CAMUNDONGOS COM RETOCOLITE
ULCERATIVA AGUDA E CRÔNICA INDUZIDA POR
DEXTRAN SULFATO DE SÓDIO**

Tese apresentada ao Programa de Pós-graduação em Patologia Experimental da Universidade Estadual de Londrina, como requisito parcial para obtenção do título de Doutor.

Orientador: Prof. Dr. Eduardo José de Almeida Araújo

Londrina
2021

Ficha de identificação da obra elaborada pelo autor, através do Programa de Geração Automática do Sistema de Bibliotecas da UEL

W324a Watanabe, Paulo da Silva.

Alterações morfológicas e fisiológicas no cólon de camundongos com retocolite ulcerativa aguda e crônica induzida por dextran sulfato de sódio / Paulo da Silva Watanabe. - Londrina, 2021.
70 f. : il.

Orientador: Eduardo José de Almeida Araújo.

Tese (Doutorado em Patologia Experimental) - Universidade Estadual de Londrina, Centro de Ciências Biológicas, Programa de Pós-Graduação em Patologia Experimental, 2021.

Inclui bibliografia.

1. Células tuft - Tese. 2. Dextran sulfato de sódio - Tese. 3. Doença inflamatória intestinal - Tese. 4. Retocolite ulcerativa - Tese. I. Araújo, Eduardo José de Almeida . II. Universidade Estadual de Londrina. Centro de Ciências Biológicas. Programa de Pós-Graduação em Patologia Experimental. III. Título.

CDU 616

PAULO DA SILVA WATANABE

**ALTERAÇÕES MORFOLÓGICAS E FISIOLÓGICAS NO
CÓLON DE CAMUNDONGOS COM RETOCOLITE
ULCERATIVA AGUDA E CRÔNICA INDUZIDA POR
DEXTRAN SULFATO DE SÓDIO**

Tese apresentada ao Programa de Pós-graduação em Patologia Experimental da Universidade Estadual de Londrina, como requisito parcial para obtenção do título de Doutor.

BANCA EXAMINADORA

Orientador: Prof. Dr. Eduardo José de Almeida
Araújo
Universidade Estadual de Londrina – UEL

Profa. Dra. Glaura Scantamburlo A. Fernandes
Universidade Estadual de Londrina – UEL

Profa. Dra. Gessilda de Alcantara Nogueira de
Melo
Universidade Estadual de Maringá – UEM

Prof. Dra. Debora de Mello Gonçalves Sant'Ana
Universidade Estadual de Maringá – UEM

Prof. Dr. Armenio Aguiar dos Santos
Universidade Federal do Ceará – UFC

Londrina, 25 de fevereiro de 2021.

AGRADECIMENTOS

A Deus, por permitir que eu concluísse mais essa etapa da minha vida e pelos momentos de dificuldade que me moldam a cada instante para ser um ser humano mais digno.

À minha amada mãe, Euseni, que me apoiou em todos os momentos, mas principalmente naqueles de angústia e desânimo.

Ao meu avô, Massao Paulo Watanabe, por todo suporte e apoio de sempre e por ter acreditado e confiado em mim.

À minha amada esposa, Carla Fioroto, por sempre estar ao meu lado me apoiando e incentivando.

Ao meu orientador, Prof. Dr. Eduardo J. A. Araújo, um exemplo que me inspira a cada dia a ser uma pessoa melhor. Muito obrigado por tudo que você me proporcionou, nunca irei esquecer.

À professora Débora de Melo Gonçalves Sant`Ana, por ser um exemplo de ser humano, a qual sempre me inspira e por ter aberto as portas para o meu Doutorado.

Aos meus colegas de laboratório, Andreia Pupim, Andreza Cavichioli, Camila Machado, Camila Baço, Matheus Deroco, Joana D`Arc, Joyce Ribeiro e Giovanni Sodré.

À Universidade Estadual de Londrina - UEL, que por meio de seu Programa de Pós-Gradual em Patologia Experimental, que me permitiu o desenvolvimento deste trabalho e a construção de conhecimento para eu me tornar Doutor em Patologia Experimental.

Ao departamento de Histologia – UEL e a todos os funcionários.

Ao *Wingate Institute for Neurogastroenterology – Queen Mary University* (Reino Unido) e ao Prof. Dr L. Ashley Blackshaw por me receberem tão bem durante meu estágio de doutorado sanduíche, em especial às minhas queridas amigas: Dra. Rubina Aktar e a Dra. Madusha Peiris.

À Coordenação de Aperfeiçoamento de Pessoal de Nível CAPES, pelo financiamento da bolsa de estudos, tanto no período que estive no Brasil como no Reino Unido.

A todos que, direta ou indiretamente, contribuíram para a realização deste trabalho.

A todos vocês, muito obrigado!

WATANABE, Paulo da Silva. **Alterações morfológicas e fisiológicas no cólon de camundongos com retocolite ulcerativa aguda e crônica induzida por dextran sulfato de sódio**. 2021. 70 f. Tese – Universidade Estadual de Londrina, Londrina, 2021.

RESUMO

A doença inflamatória intestinal é uma inflamação recorrente que afeta o trato gastrointestinal, causando alterações na motilidade colônica. A evolução dessas alterações não é completamente compreendida e possivelmente está relacionada a sintomas que aparecem em diferentes graus da inflamação intestinal. Os estudos realizados em modelos animais para avaliar motilidade colônica usualmente utilizam apenas uma porção do cólon, e logo, os resultados geralmente não refletem as alterações que ocorrem em todo o órgão. Mais estudos são necessários para avaliar o desenvolvimento da colite, investigando as alterações causadas no epitélio intestinal e na parede do cólon, no modelo agudo e crônico da doença e investigar se essas alterações morfológicas interferem na motilidade de diferentes porções do cólon. O objetivo deste estudo foi avaliar as alterações estruturais e de motilidade do cólon durante o desenvolvimento da retocolite ulcerativa (RCU) aguda e crônica induzida por DSS em camundongos C57Bl/6. Os animais foram distribuídos em 5 grupos, sendo um grupo controle e os demais grupos expostos ao DSS 3% por 2, 5, 7 dias (RCU aguda) ou 2 semanas (RCU crônica). Durante a indução da RCU, os animais foram monitorados diariamente para obter o índice de atividade da doença (IAD). Após eutanásia, os cólons foram removidos e processados para análises histológicas e para as técnicas de imunofluorescência para avaliação de células *tuft* e neurônios mioentéricos. A motilidade do cólon foi determinada usando um aparelho de manometria convencional de perfusão multilúmen. De acordo com o IAD, o modelo foi eficaz em induzir a RCU tanto de forma aguda como crônica. Houve um aumento na espessura das camadas mucosa, submucosa, dos estratos da camada muscular, na parede total e redução no número de células *tuft*. Além disso, observou-se depleção de células caliciformes e um aumento na densidade de fibras de colágeno, bem como aumento numérico de neurônios colinérgicos no plexo mioentérico dos animais com RCU crônica. Tanto a população total como as subpopulações avaliadas de neurônios mioentéricos estavam atrofiadas nos grupos com RCU. A exposição progressiva ao DSS foi acompanhada de acúmulo de ajustes no padrão de motilidade colônica. O avanço da RCU provocou, dentre outros aspectos característicos de dismotilidade, redução no número de contrações, no número de complexos motores de migração colônica e no tempo total de trânsito gastrointestinal. De uma forma geral, a inflamação progressiva fez com que as contrações se tornaram mais vigorosas nas extremidades e mais longas na região medial do cólon. Concluímos que durante o progresso da RCU induzida por DSS ocorrem alterações estruturais no cólon, incluindo aumento no número de neurônios mioentéricos colinérgicos, seguidas de variações no padrão de motilidade de diferentes regiões do cólon que, em conjunto, caracterizam dismotilidade colônica.

Palavras-chave: Células *tuft*; dextran sulfato de sódio; doença inflamatória intestinal; retocolite ulcerativa; sistema nervoso entérico.

WATANABE, Paulo da Silva. **Morphological and physiological changes in the colon of mice with acute and chronic sodium dextran sulfate-induced ulcerative colitis**. 2021. 71 p. Thesis - State University of Londrina, Londrina, 2021.

ABSTRACT

Inflammatory bowel disease is a recurrent inflammation that affects the gastrointestinal tract, causing changes in colonic motility. The evolution of these changes is not completely understood and is possibly related to symptoms that appear in different degrees of intestinal inflammation. Studies carried out on animal models to assess colonic motility usually use only a portion of the colon, and therefore, the results generally do not reflect the changes that occur in the entire organ. Further studies are needed to assess the development of colitis, investigating the changes caused in the intestinal epithelium and in the colon wall, in the acute and chronic model of the disease and to investigate whether these morphological changes interfere with the motility of different portions of the colon. The aim of this study was to evaluate the structural and motility changes of the colon during the development of acute and chronic DSS-induced ulcerative colitis (UC) in C57Bl/6 mice. The animals were assigned into 5 groups, one control group and the other groups exposed to the DSS 3% for 2, 5, 7 days (acute UC) or 2 weeks (chronic UC). During the RCU induction, the animals were monitored daily to obtain the disease activity index (IAD). After euthanasia, the colons were removed and processed for histological analysis and for immunofluorescence techniques to evaluate tuft cells and myenteric neurons. Colon motility was determined using a conventional multi-lumen perfusion manometry device. According to the IAD, the model was effective in inducing UC at both acute (up to 7 days DSS) and chronic (two weeks DSS). There was an increase in the thickness of the mucous, submucosal, muscular, in the total wall and a reduction in the number of tuft cells. In addition, depletion of goblet cells and an increase in the density of collagen fibers was observed, as well as a numerical increase of cholinergic neurons in the myenteric plexus of animals with chronic UC. Both the total population and the assessed subpopulations of myenteric neurons were stunted in the groups with UC. Progressive exposure to DSS was accompanied by an accumulation of adjustments in the colonic motility pattern. The advancement of the RCU caused, among other characteristic features of dysmotility, a reduction in the number of contractions, in the number of colonic migrating motor complex and in the total gastrointestinal transit time. In general, progressive inflammation has caused contractions to become more vigorous in the extremities and longer in the medial region of the colon. We conclude that during the progress of the DSS-induced UC, structural changes occur in the colon, including an increase in the number of cholinergic myenteric neurons, followed by variations in the motility pattern of different regions of the colon that, together, characterize colonic dysmotility.

Keywords: Inflammatory bowel; ulcerative colitis; enteric nervous system; tuft cells; dextran sodium sulfate.

LISTA DE ILUSTRAÇÕES

- Figura 1** – Prevalência global das doenças inflamatórias intestinais destacando os locais de menor e maior prevalência no ano de 2015. Fonte: adaptado de Kaplan et al. (2015).13
- Figura 2** – Fisiopatologia da retocolite ulcerativa..18
- Figura 3** – Morfologia da célula Tuft - As células tuft intestinal são facilmente distinguíveis dos enterócitos vizinhos por sua borda apical única e corpo da célula em forma oval. Os microvilos apicais conectam o ambiente extracelular do lúmen ao citoplasma intracelular através de um feixe filamentosos. Vesículas que transportam carga desconhecida são intercaladas dentro do feixe filamentosos, que termina em uma rede tubular no ápice do núcleo. Projeções laterais da membrana ou cytospinule emanam da célula do tope e perfuram a membrana dos enterócitos adjacentes. Fonte: adaptado de Banerjee et al. (2018).21
- Figura 4** – Esquema explicando a disposição dos neurônios em gânglios e plexos na parede do trato gastrintestinal (adaptado de FURNESS, 2012).23

ARTIGO

- Figura 1** – **(A)** Loss of body weight during 2 (DSS2d), 5 (DSS5d) and 7 (DSS7d) days. **(B)** Index of disease activity in DSS-induced ulcerative colitis. Effect of orally administered sodium dextran sulfate on colon edema **(C)** diameter **(D)** of the distal colon and in the total length of the colon **(E)**. Data presented as mean \pm S.E.M. (n = 10 per group) (* P < 0.05, ** P < 0.005, **** P < 0.0001, ANOVA followed by the Tukey test)46
- Figura 2** – Photomicrograph of histological sections stained by H&E. Groups: Control **(A)** DSS7d **(B)** and DSS3C **(C)**. **(D)** The arrow shows a rupture of the intestinal epithelium. **(E)** arrowhead - Inflammatory infiltrate within the ganglion. **(F)** Graph representing the distal colon's analysis of wall. Mucosa thickness (Muc), crypt depth

(crypt), submucosa (sub), circular muscle (Circ. Mu.), Longitudinal muscle (Long. Mu.), Total muscle (Total Mu.) were analyzed. Histological sections of the distal colon stained with PAS from mice in the control group (**H**) and exposed to the DSS for 7 (DSS7d) days (**I**) and the group with chronic colitis (DSS3C) (**J**) and in (**G**) Graph representative. Arrow points to goblet cells. Type I (**L**) and III (**M**) collagen quantification using Sirius Red staining. Data presented as mean \pm S.E.M. (n = 5 per group) (* $P < 0.05$, *** $P < 0.005$, **** $P < 0.0001$, ANOVA followed by the Tukey test).....47

Figura 3 – (**A**) Number of tuft cells in mice's total colon exposed to DSS for 2 (DSS2d), 5 (DSS5d), 7 (DSS7d) days and also in the group induced to chronic ulcerative colitis (DSS3C) and number of tuft cells in the proximal (**B**) and distal (**C**) colon. Data presented as mean \pm S.E.M. (n = 5 per group) (* $P < 0.05$, ** $P < 0.01$, *** $P < 0.005$. ANOVA followed by the Tukey test).48

Figura 4 – Representative graph of neuronal distribution (**A**) and morphometry (**B**) of neurons of general population (PGP 9.5), nitrenergic (nNOS) and cholinergic (ChAT) positive. (**C**) ChAT x PGP 9.5 ratio and (**D**) nNOS x PGP 9.5 ratio of control mice and exposed to DSS for 7 (DSS7d) days and group with chronic colitis (DSS3C). Data presented as mean \pm S.E.M. (n = 5 per group) (* $P < 0.05$, ** $P < 0.01$, ANOVA followed by the Tukey test).....49

Figura 5 – Representative photomicrograph showing the PGP 9.5 +, nNOS + and ChAT + neurons of control group and groups exposed to DSS for 7 days (DSS7d) and chronic colitis (DSS3C).50

Figura 6 – Representative graph of the colonic manometry, comparing control group and groups exposed to the DSS for 7 (DSS7d) days and with chronic colitis (DSS3C). Analyzed parameters: Amplitude of contractions (**A**), area under the curve (AUC) (**B**) and frequency [number (Nb) that spontaneous contractions occurred, quantified in four categories in the proximal colon (**C**), Proximal Medium (**D**), Medial Distal (**E**) and Distal (**F**). Data presented as mean \pm S.E.M.

(n = 10 per group) (* $P < 0.05$, ANOVA followed by the Tukey test).....51

Figura 7 – Representative graph of the colonic manometry, comparing control group and groups exposed to the DSS for 7 (DSS7d) days and with chronic colitis (DSS3C). The duration of spontaneous contractions **(A)**. The percentage of time the colon remained contracted **(B)**. **(C)** the relaxation time between contractions and the percentage of time the colon remained quiescent **(D)** was calculated. The duration of contractions were categorized and quantified [number (Nb) in the proximal **(E)**, middle proximal **(F)**, distal **(G)** and distal **(H)** colon. Data presented as mean \pm S.E.M. (n = 10 per group) (* $P < 0.05$, ANOVA followed by the Tukey test).....52

Figura 8 – Colonic migratory motor complex (CMMC) profile in mice with acute (DSS7d) and Chronic (DSS3C) colitis. **A:** Plot showing the CMMCs number in 30min. **B:** Average time duration of each CMMC. **C:** Average quiescent time (s) between CMMCs. **D:** Classification of direction and Number (Nb) of CMMCs in 30min. Data presented as mean \pm S.E.M. (n = 10 per group) (* $P < 0.05$; ** $P < 0.01$; *** $P < 0.005$, ANOVA followed by the Tukey test).....53

LISTA DE TABELAS

Tabela 1 – Classificação dos modelos experimentais de doença inflamatória intestinal de acordo com a especificação, para retocolite ulcerativa ou doença de Chron.....25

ARTIGO

Tabela 1 – Organization of groups to induce UC with DSS in drinking water.....45

Tabela 2 – Primary and secondary antibodies used for the immunofluorescence technique.....45

LISTA DE ABREVIATURAS E SIGLAS

°C	Graus Celcius
ACh	Acetilcolina
AUC	<i>Area under the curve</i>
ChAT	Colina acetiltransferase
CMMC	<i>Colonic Migrating Motor Complex</i>
DC	Doença de Crohn
DII	Doença inflamatória intestinal
DSS	Dextrano sulfato de sódio
Fig	Figura
DAI	<i>Disease activity index</i>
IAD	índice de atividade da doença
IBD	<i>Inflammatory Bowel Disease</i>
IFNs	Interferons
IL	Interleucina
MC	Muscular circular
ML	Muscular Longitudinal
NF-κB	Fator nuclear κB
NO	Oxido Nítrico
PAS	Ácido periódico de Schiff
PBS	Tampão fosfato-salina
PFA 4%	Paraformaldeído 4%
PRRs	Receptor de reconhecimento de padrões
RCU	Retocolite ulcerativa
SNE	Sistema nervoso entérico
TGI	Trato gastrointestinal
TLRs	Receptores do tipo Toll
TNBS	ácido trinitrobenzeno sulfônico
TNF	Fatore de Necrose Tumoral

SUMÁRIO

1	INTRODUÇÃO	13
1.1	DOENÇAS INFLAMATÓRIAS INTESTINAIS.....	13
1.2	RESPOSTA IMUNOLÓGICA	16
1.3	SISTEMA DIGESTÓRIO.....	19
1.4	MODELOS EXPERIMENTAIS PARA RCU.....	25
2	OBJETIVO	28
2.1	OBJETIVO GERAL.....	28
2.2	OBJETIVOS ESPECÍFICOS.....	28
3	ARTIGO CIENTÍFICO - COLONIC MOTILITY ADJUSTMENTS IN ACUTE AND CHRONIC DSS-INDUCED COLITIS	28
4	CONSIDERAÇÕES FINAIS	55
5	REFERÊNCIAS	56
	ANEXOS	63
	A – Aprovação CEUA	64
	B – Normas da Revista Neurogastroenterology and Motility	65

1. INTRODUÇÃO

1.1 Doenças Inflamatórias Intestinais

Atualmente na literatura são descritas diferentes doenças inflamatórias que acometem o intestino delgado e grosso. A doença inflamatória intestinal (DII), do inglês *Inflammatory Bowel Disease* (IBD), refere-se às doenças inflamatórias crônicas do trato gastrointestinal, incluindo a retocolite ulcerativa (RCU) e a doença de Crohn (DC) (ACTIS et al., 2019).

A DII ocorre em todo o mundo, embora seja mais comum em países ocidentais, a europa, américa do norte e a oceania são os locais onde se encontra o maior número de casos diagnosticados, com taxas de incidência de 4 a 10 casos para cada 100.000 habitantes por ano e taxas de prevalência entre 40 a 100 para cada 100.000 habitantes (Figura 1) (ALATAB et al., 2020; KAPLAN, 2015).

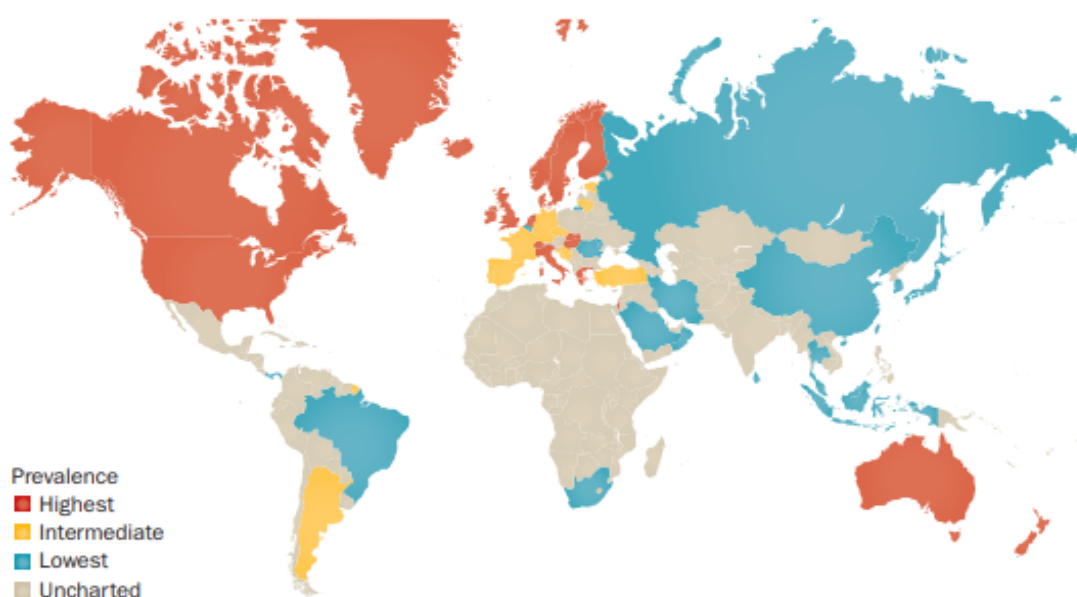


Figura 1. Prevalência global das doenças inflamatórias intestinais destacando os locais de menor e maior prevalência no ano de 2015. Fonte: adaptado de Kaplan et al. (2015).

Acredita-se que a menor incidência em outras partes do mundo esteja relacionada a hábitos alimentares, estilo de vida ou problemas técnicos de diagnóstico da doença (HENDRICKSON; GOKHALE; CHO, 2002). No Brasil, entre o ano de 1986 e 1990, foi registrado um caso para cada 100.000 mil habitantes, já entre 2001 e 2005 esse número subiu para 4,5 casos para cada 100.000 habitantes (KAPLAN, 2015).

22 Em São Paulo, um estudo mostrou que o número de novos casos dobrou de 4,5
23 por 100.000 habitantes em 1995 para 9,5 casos em 2001-2005. Ambos os sexos são
24 afetados (VICTORIA; SASSAK; NUNES, 2009). Um levantamento realizado em 2017
25 mostrou que todo dia no Brasil uma pessoa é diagnosticada com DII (CURY;
26 OLIVEIRA; CURY, 2019).

27 O impacto econômico destas doenças é sem dúvidas um fato preocupante.
28 Estima-se que os gastos diretos e indiretos possam chegar até 8 bilhões nos EUA e
29 12 bilhões na Europa de dólares por ano (GOYAL et al., 2014).

30 A DII é mais comumente diagnosticada entre a terceira e a quarta década de vida,
31 sem diferença observada entre homens e mulheres. Aproximadamente 20% de todos
32 os pacientes com DII desenvolvem sintomas durante a infância (ROGERS; CLARK;
33 KIRSNER, 1971), com cerca de 5% sendo diagnosticados antes dos 10 anos de idade
34 (MIR-MADJLESSI; MICHENER; FARMER, 1986). Cerca de 25% das crianças
35 afetadas têm um histórico familiar positivo de DII (GILAT et al., 1987). Ainda em
36 relação à idade, a RCU apresenta padrão de incidência bimodal, com o pico de início
37 entre 20 e 30 anos e um segundo pico menor entre 60 e 70 anos de idade (MALIK,
38 2015).

39 Em pacientes com DII pode ocorrer manifestações extra intestinais, como em: a)
40 articulações periféricas e axiais: artralgia, artrite periférica, sacroiliite e espondilite
41 anquilosante; b) pele e mucosas: eritema nodoso, pioderma gangrenoso e aftas orais;
42 c) fígado: hepatite autoimune e colangite esclerosante primária; e d) olhos: episclerite
43 e uveíte (NIKOLAUS; SCHREIBER, 2007).

44 A fisiopatologia da DII é complexa e ainda não está totalmente elucidada. A
45 literatura aponta que em indivíduos geneticamente susceptíveis vários fatores
46 ambientais (DANESE; SANS; FIOCCHI, 2004) e alterações na composição da
47 microbiota intestinal (NAGAO-KITAMOTO et al., 2016), ingestão alimentar inadequada,
48 estresse psicológico e a utilização de fármacos anti-inflamatórios podem ser os
49 gatilhos de distúrbios nas respostas imunológicas inatas e adaptativas do trato
50 gastrointestinal (TGI), os quais provocam o surgimento e a modulação dessas
51 doenças (KNIGHTS; LASSEN; XAVIER, 2013).

52 A DC, ao contrário da RCU, pode envolver qualquer parte do trato gastrointestinal
53 desde a orofaringe até a área perianal. Os segmentos acometidos frequentemente
54 são intercalados por porções de tecidos normais. A inflamação pode ser transmural,
55 muitas vezes se estendendo até a serosa, resultando em vias sinusais ou formação

56 de fístula. Os achados histológicos incluem pequenas ulcerações superficiais e
57 inflamação crônica focal que se estende até a submucosa, às vezes acompanhada
58 por formação de granuloma não causador de câncer. A localização mais comum é a
59 região ileocecal, seguida apenas pelo íleo terminal, intestino delgado difuso ou doença
60 colônica isolada em ordem decrescente de frequência (HENDRICKSON; GOKHALE;
61 CHO, 2002).

62 A DC e a RCU diferem entre si por possuírem aspectos fisiopatológicos, clínicos,
63 e terapêuticos inerentes a cada uma delas (BETTERIDGE et al., 2013; DIGNASS et
64 al., 2012; VAN ASSCHE et al., 2010). Em alguns casos não é possível diferenciar a
65 DC e a RCU, como por exemplo casos de colite que apresentam elementos clínicos,
66 endoscópicos e anatomopatológicos das duas doenças. Estes casos são classificados
67 como colite indeterminada ou colite não classificada (BAUMGART; SANDBORN,
68 2007).

69 A DC e a RCU podem também se desenvolver por herança genética
70 (SPEHLMANN et al., 2008). Há descrito na literatura que ao menos 110 loci
71 genéticos são relacionados a susceptibilidade tanto para DC quanto para RCU; 30
72 loci são específicos para DC e 23 para RCU (VERMEIRE; RUTGEERTS, 2013).

73 Em média os pacientes com RCU possuem de 5,7 a 15,5% parentes de primeiro
74 grau com a mesma doença (ORDÁS et al., 2012), também a ocorrência em gêmeos
75 monozigóticos é extremamente alta, sendo aproximadamente 800 vezes maior que
76 na população geral (CHILDERS et al., 2014).

77 A RCU é uma condição na qual a resposta inflamatória e as alterações
78 morfológicas permanecem confinadas ao cólon e reto. O reto está envolvido em 95%
79 dos pacientes, com graus variáveis de extensão proximal. A inflamação é limitada
80 principalmente à mucosa e consiste no envolvimento contínuo de gravidade variável
81 com ulceração, edema e hemorragia ao longo do cólon e reto. Os achados
82 histológicos característicos são inflamação aguda e crônica da mucosa por leucócitos
83 polimorfonucleares e células mononucleares, abscessos de cripta, distorção das
84 glândulas mucosas e depleção de células caliciformes (HENDRICKSON; GOKHALE;
85 CHO, 2002).

86 Para o diagnóstico da RCU deve-se realizar uma colonoscopia com análise
87 anatomopatológica de biópsias do reto e cólons. Os achados endoscópicos incluem:
88 perda do padrão vascular submucoso, eritema, granulosidade, friabilidade erosões,
89 ulcerações e sangramento espontâneo (FORD; MOAYYEDI; HANAUER, 2013).

90 1.2 Resposta imunológica

91

92 As respostas imunes inata e adaptativa são os dois tipos de classes efetoras do
93 sistema imunológico. A resposta imune inata atua como uma primeira linha de defesa
94 e fornece proteção inespecífica, enquanto a resposta imune adaptativa é altamente
95 específica por natureza e é ativada pela imunidade inata (ABUL ABBAS ANDREW H.
96 LICHTMAN SHIV PILLAI, 2018).

97 São componentes da imunidade inata a barreira epitelial, neutrófilos, macrófagos,
98 células dendríticas, células assassinas naturais (células NK) etc. Essa forma de
99 imunidade é ativada pelos agentes microbianos reconhecidos pelos receptores de
100 reconhecimento de padrões, receptores do tipo Toll (TLRs) e receptores do tipo NOD
101 (PASTORELLI et al., 2013). Os neutrófilos, juntamente com outras células, iniciam a
102 inflamação liberando citocinas pró-inflamatórias, como TNF- α , IL-1, IL-6 e IL-8, que
103 ativam ainda mais a resposta imune adaptativa (WALLACE, 2014).

104 O sistema imunológico adaptativo compreende linfócitos T e células B que na
105 ativação liberam citocinas e anticorpos (ABUL ABBAS et al., 2018). Pensa-se que as
106 células T sejam o principal contribuinte da DII devido ao aumento da liberação de
107 mediadores pró-inflamatórios. As células Th-1 produzem uma grande quantidade de
108 interferons (IFNs), induzidas pela interleucina 12 (IL-12), e causam a patogênese em
109 pacientes com DC. Por outro lado, as células Th-2 estão envolvidas na produção de
110 IL-4, IL-5 e IL-13 e causam inflamação em pacientes com RCU (ZHANG, 2014).

111 Há ainda um terceiro tipo de célula T-auxiliar que também está envolvido na
112 patogênese da DII, isto é, as células Th-17 (SIEGMUND; ZEITZ, 2011). Essas células
113 produzem IL-17 e IL-22, ambas citocinas pró-inflamatórias capazes de promover a
114 destruição local do tecido (SIEGMUND; ZEITZ, 2011). Essas citocinas aumentam
115 ainda mais a permeabilidade intestinal, rompendo a barreira epitelial e resultando em
116 inflamação descontrolada (GOYAL et al., 2014).

117 Existem certas diferenças no perfil mediador inflamatório da CD e RCU, como IL-
118 2 e IFN- γ são responsáveis pela inflamação na CD, enquanto IL-4, IL-5 e IL-10 estão
119 envolvidas na patogênese da RCU (MONTELEONE et al., 2002). A concentração
120 desses mediadores é altamente elevada no sangue, fezes e mucosa intestinal de
121 pacientes com DII (GOYAL et al., 2014). A liberação dessas células inflamatórias é
122 regulada por diferentes vias envolvidas na inflamação, ou seja, via fator nuclear κ B
123 (NF- κ B) e MAPK e via JAK/STAT (PEDERSEN, 2014).

124 O NF- κ B e as MAPK (*Mitogen Activated Protein Kinases* - Proteíno-quinases
125 ativadas por mitógenos) são ativadas pelos TLR-4 que estimulam ainda mais a
126 liberação de TNF- α , IL-6 e IL-12 por meio de macrófagos, exacerbando a resposta
127 inflamatória (COSKUN et al., 2011). Além disso, as citocinas exercem sua sinalização
128 ativando a via JAK/STAT, que está envolvida na produção de várias interleucinas.
129 JAK, quando fosforilam proteínas STAT, translocam-se do citoplasma para o núcleo
130 para alterar a expressão gênica dos genes alvo (COSKUN et al., 2013). A liberação
131 de mediadores pró-inflamatórios por essas vias resulta na progressão da doença (WU
132 et al., 2016).

133 Naturalmente, em condições saudáveis o sistema imune do TGI mantém estável
134 equilíbrio com a microbiota, respondendo apenas de modo controlado aos antígenos
135 provenientes da dieta, condição denominada tolerância imunológica. Desta forma, a
136 RCU pode ocorrer devido a quebra desta tolerância, mencionado anteriormente,
137 levando assim a resposta imune inadequada, demasiada, contra bactérias comensais
138 não patogênicas (GOYAL et al., 2014).

139 Os antígenos oriundos do lúmen intestinal ativam a resposta imune inata por meio
140 da interação com macrófagos e células dendríticas residentes na lâmina própria.
141 Estes, por sua vez, apresentam os antígenos para os linfócitos B e T, desencadeando
142 assim a ativação da resposta imune adaptativa (ORDÁS et al., 2012). Como pode ser
143 observado na figura 2, as células dendríticas podem ainda abrir as junções oclusivas
144 presentes entre as células epiteliais e projetar seus prolongamentos para a luz do
145 órgão e entrar em contato direto com fragmentos bacterianos do lúmen (NIESS, 2005).

146 Os macrófagos residentes exercem papel fundamental na manutenção da
147 homeostasia do intestino. São células importantes para atividade bactericida e
148 fagocitose, e também produzem e liberam mediadores anti-inflamatórios (SWIRSKI et
149 al., 2009).

150 Os macrófagos humanos possuem características fenotípicas singulares e vias de
151 sinalização distintas das encontradas nos monócitos do sangue periférico (SMYTHIES
152 et al., 2010). Ou seja, após a estimulação de PRR, como os TLR, alguns macrófagos
153 intestinais não secretam citocinas pró-inflamatórias, isto é, secretam seletivamente

154 citocinas anti-inflamatórias (IL-10), que ajudam na resolução do processo inflamatório
 155 intestinal (DENNING et al., 2007).

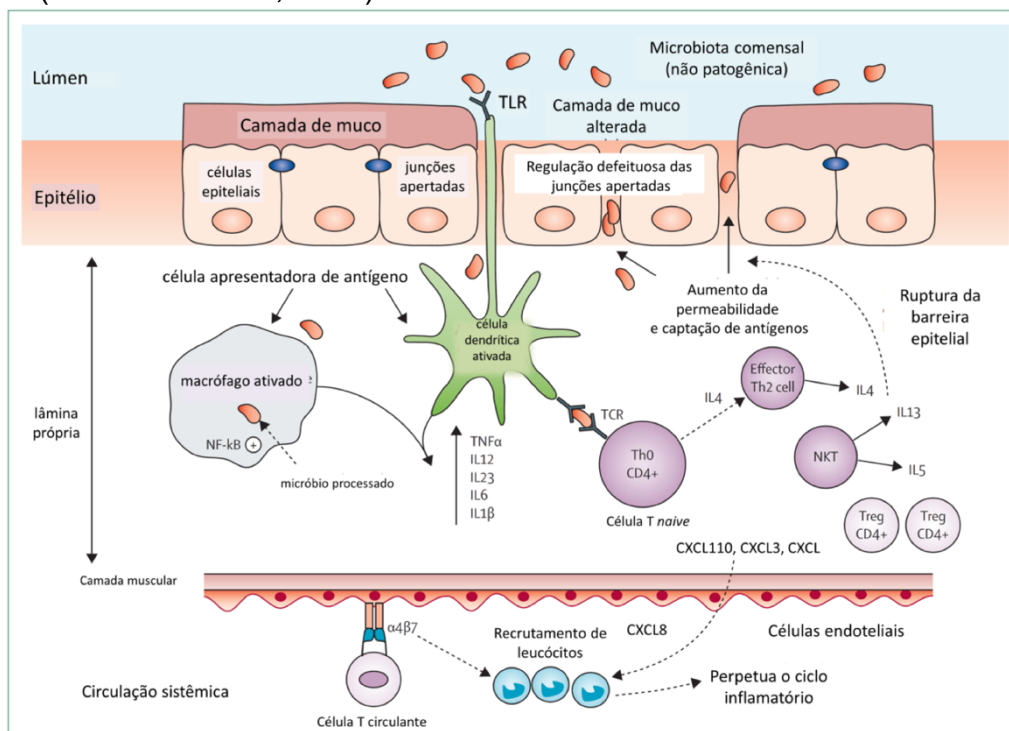


Figura 2. Fisiopatologia da retocolite ulcerativa - A ruptura das junções oclusivas e a camada de muco que cobre o epitélio causa o aumento da permeabilidade intestinal, resultando em aumento da captação de antígenos luminiais. Macrófagos e células dendríticas no reconhecimento de bactérias não patogênicas por meio de receptores de reconhecimento de padrões, alteram seu status funcional de tolerogênico para um fenótipo ativado. A ativação das vias NF-κB estimula a transcrição de genes pró-inflamatórios, resultando no aumento da produção de citocinas pró-inflamatórias. Após o processamento de antígenos, macrófagos e células dendríticas as apresentam para células T CD4 naive, promovendo diferenciação em células efectoras Th2, caracterizadas pela produção de IL-4. As células T natural-killers são a principal fonte de interleucina 13, que tem sido associada a ruptura da barreira celular epitelial. As células T circulantes portadoras de integrina-α4β7 se ligam às células endoteliais que estão expressando muitas moléculas de adesão endotelial, levando ao aumento da entrada de células T específicas do intestino na lâmina própria. Fonte: adaptado de Ordás (2012).

156 Na mucosa de pacientes com RCU, o equilíbrio homeostático entre as células T
 157 reguladoras e efectoras (*T-helper* [Th] 1, Th2 e Th17) está alterado. A RCU está
 158 associada a uma resposta Th2 (células do tipo *T helper*, do inglês *T auxiliares*), atípica
 159 mediada por células NK não clássicas que produzem IL-5 e IL-13 (WU et al., 2016).

160 A IL-13, possui papel primordial, pois exerce função citotóxica contra as células
 161 epiteliais, incluindo indução de apoptose e alteração na composição das proteínas de
 162 junção epitelial amplificando a lesão tecidual. Haja visto que com estudos que fizeram
 163 o bloqueio da IL-13 e a depleção de células T foi possível prevenir o desenvolvimento
 164 da colite (HELLER et al., 2005, 2008).

165

166 1.3 Sistema digestório

167

168 O sistema digestório é constituído pelo tubo digestório e glândulas anexas, que
169 realizam a ingestão, mastigação, deglutição e digestão do alimento e absorção dos
170 nutrientes, além da eliminação dos restos não digeridos. O tubo digestório é a porção
171 responsável por macerar, encaminhar, digerir, seleccionar e absorver os elementos
172 nutritivos e a água, sendo subdividido em esôfago, estômago, intestino delgado e
173 intestino grosso. No humano o intestino delgado é formado pelo duodeno, jejuno e
174 íleo que possuem as funções de digestão e absorção dos nutrientes, enquanto o
175 intestino grosso é formado pelo ceco, colos ascendente, transverso, descendente e
176 sigmoide seguido do reto e do canal anal que fazem a absorção de eletrólitos e água,
177 além de formarem o bolo fecal (SANT'ANA; MIRANDA-NETO; OLIVEIRA, 2006). Em
178 ratos o sistema digestório é muito semelhante ao humano, possuindo a mesma
179 nomenclatura anatômica do esôfago ao íleo, sendo o intestino grosso dividido em ceco,
180 cólon proximal, cólon distal, reto e canal anal (JOAN, 1979).

181 O intestino delgado é formado histologicamente por: túnica mucosa, tela
182 submucosa, túnica muscular e túnica serosa. A túnica mucosa é altamente
183 vascularizada e composta pelo epitélio, lâmina própria e muscular da mucosa. Na
184 mucosa são encontrados os vilos, que são projeções da lâmina própria em direção ao
185 lúmen intestinal, que estão recobertas por um epitélio de revestimento simples
186 prismático; além de invaginações epiteliais nos espaços intervillares que formam
187 numerosas glândulas, denominadas de criptas intestinais (JUNQUEIRA; CARNEIRO,
188 2008). As criptas são glândulas simples e tubulares que circundam a base dos vilos e
189 se abrem como perfurações do revestimento interno do intestino (JUNQUEIRA LC,
190 2008).

191 No epitélio intestinal as células mais numerosas são os enterócitos, de formato
192 colunar, com aproximadamente 25 μm de altura, com núcleo oval localizado no polo
193 basal e com uma borda em escova (microvilosidades) no polo apical. Essas células
194 são responsáveis pela digestão terminal de macromoléculas e absorção de água e
195 nutrientes, além de modificar ácidos graxos em triglicerídeos, formando quilomícrons,
196 e transportar nutrientes para vasos sanguíneos e linfáticos da lâmina própria, de onde
197 serão distribuídos para todo o corpo (JUNQUEIRA LC, 2008).

198 Células caliciformes também estão presentes no epitélio intestinal, são glândulas
199 unicelulares com formato de cálice, com a base apoiada na lâmina basal e polo apical

200 repleto de gotículas secretoras revestidas por membranas voltadas para o lúmen
201 intestinal, de modo a deslocar o citoplasma para a periferia da célula e o núcleo para
202 o polo basal. Essas células possuem a função de produzir e secretar o mucinogênio,
203 cuja forma hidratada é a mucina, componente fundamental do muco que reveste o
204 lúmen intestinal. O muco lubrifica e protege o epitélio contra a abrasão e ação da
205 microbiota intestinal, embora também sirva como fonte de nutrientes para esses
206 microrganismos (GARTNER LP, 2003).

207 Ainda no epitélio intestinal está presente um tipo celular muito singular, as células
208 tuft (GERBE; JAY, 2016). Em camundongos adultos, as células Tuft representam
209 0,4% de todas as células epiteliais (GERBE et al., 2011). Este tipo celular apresenta
210 características morfológicas bastante singulares como demonstrado na figura 3, possui
211 uma volumosa quantidade de microvilosidade apicais mais altas do que as dos
212 enterócitos e que se organizam para formar uma borda em escova, e esta
213 característica propicia uma aparência de um “tufo” (GERBE; JAY, 2016). A morfologia
214 deste tipo celular sofre variações dependendo de sua localização: no trato respiratório
215 assumem um formato achatado (MEYRICK; REID, 1968), na vesícula biliar uma forma
216 cuboide (LUCIANO; GROOS; REALE, 2003) e no intestino apresentam um corpo
217 cilindro que se estreita nas extremidades apicais e basais (BANERJEE et al., 2018).

218 Os cytospinule das células Tuft são estruturas morfológicas únicas e inerentes a
219 este tipo celular, são 3-4 projeções laterais que perfuram a membrana da célula
220 vizinha e podem fazer contato direto com a membrana nuclear desta célula (figura 3).
221 Acredita-se que os cytospinule funcionem como um meio direto de comunicação e
222 transporte de carga (HOOVER et al., 2017).

223

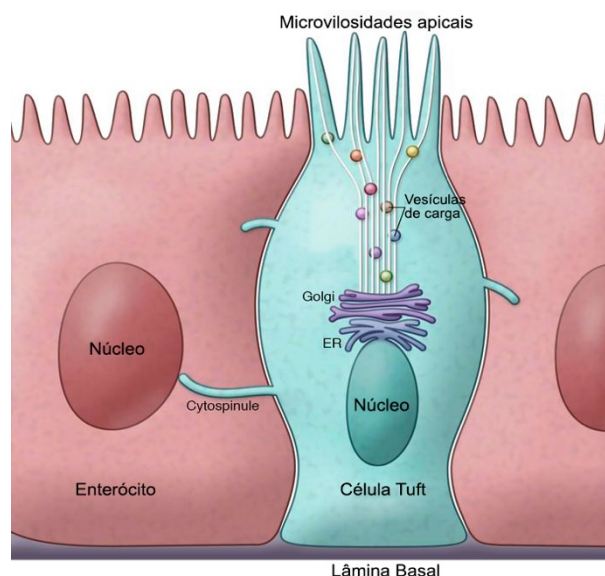


Figura 3. Morfologia da célula Tuft - As células tuft intestinal são facilmente distinguíveis dos enterócitos vizinhos por sua borda apical única e corpo da célula em forma oval. Os microvilos apicais conectam o ambiente extracelular do lúmen ao citoplasma intracelular através de um feixe filamentososo. Vesículas que transportam carga desconhecida são intercaladas dentro do feixe filamentososo, que termina em uma rede tubular no ápice do núcleo. Projeções laterais da membrana ou cytospinule emanam da célula Tuft e perfuram a membrana dos enterócitos adjacentes. Fonte: adaptado de Banerjee et al. (2018).

224

225 As células Tuft desempenham papel imunológico importante nas infecções
 226 parasitárias, alguns trabalhos demonstraram que diferentes parasitos induziram
 227 hiperplasia de células Tuft (GERBE; JAY, 2016; VON MOLTKE et al., 2016). A citocina
 228 IL-25 desempenha papel fundamental na imunidade Th2 (BANERJEE et al., 2018).
 229 Por meio de imunohistoquímica foi observado que as células Tuft expressam IL-25 de
 230 maneira constitutiva, citocina inexistente nas demais célula do epitélio intestinal
 231 (GERBE; JAY, 2016). A citocina IL-13 desempenha papel direto na hiperplasia das
 232 células Tuft, uma vez que animais nocautes para IL-13 não desenvolveram hiperplasia
 233 dessas células após infecções parasitárias, por outro lado quando a IL-13 foi
 234 administrada de maneira exógena, houve indução de hiperplasia tanto in vitro como
 235 in vivo das células Tuft (VON MOLTKE et al., 2016).

236 As células Tuft também possuem importante papel na neuromodulação, uma vez
 237 que tem sido demonstrando que esse tipo celular é fonte não neural de acetilcolina
 238 (Ach) e estas por sua vez se encontram extremamente perto dos neurônios do sistema
 239 nervoso entérico (SNE) (MIDDELHOFF et al., 2017). Desde a década de 1990 a
 240 ocorrência de células imunorreativas para colina acetiltransferase (ChAT) no epitélio
 241 da mucosa do intestino grosso humano já era relatada (COSTA et al., 1996).

242 A lâmina própria situa-se abaixo do epitélio intestinal e é constituída de tecido
243 conjuntivo frouxo, abrigando diversos vasos sanguíneos e linfáticos de pequeno
244 calibre, além de envolver externamente glândulas e nódulos linfáticos ocasionais. A
245 muscular da mucosa circunda a lâmina própria, delimitando a mucosa e a submucosa.
246 Ela é composta por células musculares lisas reunidas em uma camada circular interna
247 e uma longitudinal externa que são responsáveis por desenvolverem contrações
248 rítmicas que movimentam os vilos de forma intensa durante a digestão (GARTNER
249 LP, 2003).

250 A tela submucosa é formada por tecido conjuntivo denso fibroelástico não-
251 modelado com a presença de numerosos vasos sanguíneos e linfáticos de maior
252 calibre (arteríolas e vênulas). Nesta tela ainda se encontra o plexo submucoso,
253 componente nervoso que controla a motilidade da mucosa, a atividade secretora das
254 glândulas e a vasomotricidade (JUNQUEIRA LC, 2008).

255 A túnica muscular é formada por dois estratos de músculo liso: o estrato circular
256 da túnica muscular (MC) disposta mais próxima do lúmen, e o estrato longitudinal da
257 túnica muscular (ML) disposta mais periférico do lúmen. Essas fibras musculares são
258 responsáveis pela atividade motora intestinal. Entre os dois estratos da túnica
259 muscular situa-se o plexo mioentérico, outro componente nervoso que regula a
260 atividade peristáltica, bem como outros tipos de movimentos exercidos pela túnica
261 muscular. A túnica serosa é formada por tecido conjuntivo frouxo que recobre
262 externamente todo o tubo intestinal. Essa túnica é chamada de serosa quando o
263 segmento do tubo digestório é revestido por peritônio, e conhecida como adventícia
264 quando o segmento é retroperitoneal, como é o caso do esôfago (JUNQUEIRA LC,
265 2008).

266 O sistema digestório possui um sistema nervoso intrínseco, denominado Sistema
267 Nervoso Entérico (SNE), que controla todas as funções digestórias. O SNE é a maior
268 e mais complexa divisão do sistema nervoso autônomo em vertebrados. Distribuído
269 por todo o TGI, vesícula biliar e o pâncreas, é organizado como uma rede
270 interconectando neurônios e células da glia agrupados no interior de gânglios,
271 localizados nos dois maiores plexos: mioentérico e o plexo submucoso, demonstrados
272 na figura 4 (FURNESS; COSTA, 1987).

273

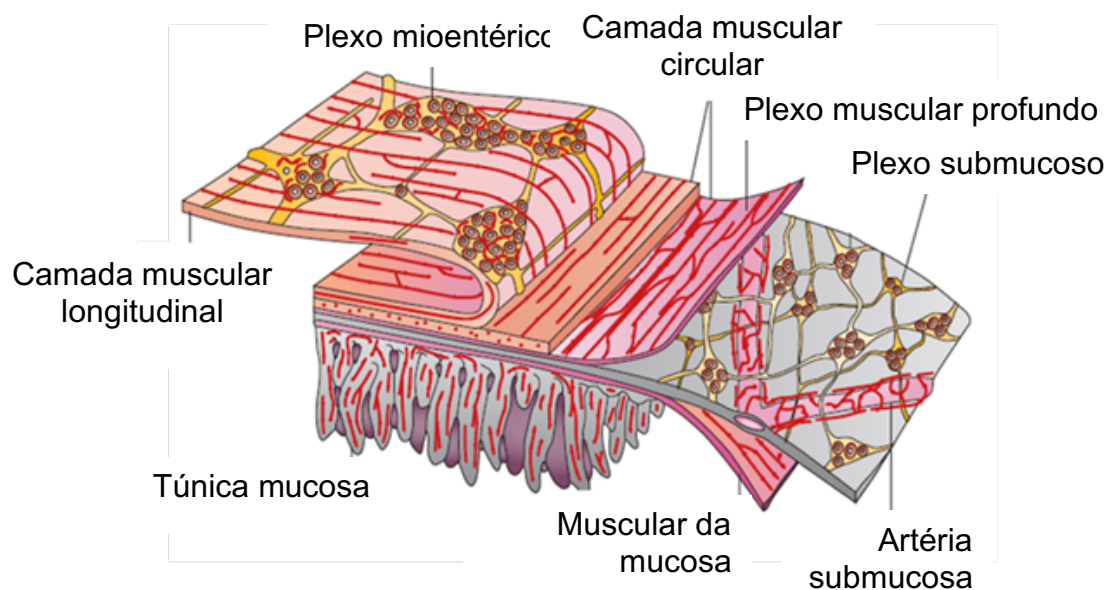


Figura 4. Esquema explicando a disposição dos neurônios em gânglios e plexos na parede do trato gastrointestinal (adaptado de FURNESS, 2012).

274

275 Os plexos ganglionados são o mioentérico e o submucoso, dos quais emergem
 276 feixes de fibras nervosas que formam os plexos não-ganglionados, presentes em toda
 277 a parede intestinal (FURNESS JB, 2006).

278 Além de neurônios, no SNE existem também as Células da Glia Entérica, que
 279 possuem diversas funções ligadas a sobrevivência neuronal, como apoio metabólico,
 280 estrutural, trófico e de proteção (RUHL; NASSER; SHARKEY, 2004).

281 O SNE é formado por vários tipos de neurônios comparáveis em número ao da
 282 medula espinal (80-100 milhões) e com uma série de neurotransmissores e
 283 neuromoduladores semelhantes aos encontrados no sistema nervoso central. Com
 284 base nas propriedades eletrofisiológicas e histoquímicas podem ser classificados em
 285 subpopulações funcionalmente distintas, incluindo neurônios aferentes primários
 286 intrínsecos, interneurônios, neurônios motores, neurônios intestinofugais, neurônios
 287 secretores e vasomotores (FURNESS, 2012).

288 A maior parte dos neurônios mioentéricos humanos são colinérgicos ou
 289 nitrérgicos. Os neurônios nitrérgicos humanos parecem ser interneurônios
 290 descendentes ou neurônios motores inibitórios. Por outro lado, os neurônios
 291 mioentéricos colinérgicos são neurônios motores excitatórios (FURNESS JB, 2006).

292 A motilidade colônica depende do SNE para propulsão do conteúdo. A motilidade
293 colônica funciona inadequadamente quando o SNE do colón distal e do reto está
294 ausente congenitamente em pacientes com doença de Hirschsprung, por exemplo
295 (SWENSON, 2002), ou quando o SNE sofre alguma degeneração mais tarde na vida,
296 como na doença de Chagas (MATSUDA; MILLER; EVORA, 2009). Em indivíduos
297 saudáveis, os reflexos propulsivos do cólon distal e reto são regulados por centros de
298 controle central que mantêm a continência fecal e, quando apropriado, desencadeiam
299 a defecação por meio de comandos centrais retransmitidos pelo centro de defecação
300 na medula espinal lombossacral (DE GROAT et al., 1981; LYNCH et al., 2001).

301 Para haver a peristalse intestinal, uma série de eventos, e comunicação inter
302 neuronal deve ocorrer. Quando ocorre um estímulo no lúmen intestinal, células
303 enteroendócrinas podem sinalizar, secretando seus hormônios na lâmina própria,
304 estes hormônios por sua vez irão ativar os neurônios aferentes primários que então
305 ativarão um interneurônio. Estímulos de estiramento também podem ativar os
306 interneurônios mecanossensoriais ascendentes e descendentes por si só, não
307 dependendo então de outra célula para sinalizar (SPENCER et al., 2016). Os
308 interneurônios ascendentes ativam neurônios motores excitatórios na ML e na MC.
309 Os interneurônios descendentes ativam os neurônios motores inibitórios na ML e no
310 MC (SMITH et al., 2007).

311 Os neurônios motores excitatórios da ML e MC liberam ACh para evocar contração
312 no músculo. Já os neurônios motores inibitórios da ML e da MC liberam NO e NO/ATP,
313 respectivamente, para promover um relaxamento do músculo (FURNESS, 2012).
314

315 1.4 Modelos experimentais para RCU

316 Como a etiologia exata da DII ainda é incerta, vários modelos experimentais
 317 utilizando animais foram desenvolvidos nas últimas décadas para estudar o possível
 318 mecanismo envolvido na fisiopatologia da doença e novos alvos terapêuticos. Os
 319 diferentes tipos de modelos animais são desenvolvidos para o estudo da DII (Tabela
 320 1).

Categoria	Especificidade	
	RCU	DC
Modelos quimicamente induzidos	DSS TNBS/DNBS Oxazolona Ácido acético Carragenina Iodoacetamida	TNBS/DNBS Indometacina
Modelo imunológico	2, 4-Dinitroclorobenzeno (DNCB)	
Modelos induzidos por bactérias	Induzida por <i>Salmonella</i> <i>E. coli</i> invasiva aderente	
Modelos espontâneos		Modelo de camundongos C3H/HeJBir Modelo de camundongos SAMP1/4it
Modelos geneticamente modificados	TGF- β -/ IL-2 -/ MDR1A -/ Gai2 -/ TCRa -/ XBP1 -/ NEMO -/	IL-10 -/ NOD2 -/ A20 -/ IL-23 -/ NEMO -/
Modelos de camundongos transgênicos	camundongo IL-7 Tg HLA-B27	STAT 4 HLA-B27 Camundongos DNN Caderina Tg
Modelos knock-in de mutação		TNF Δ ARE
Modelos de transferência adotiva	Modelo de alta transferência CD45RB	Modelo de alta transferência CD45RB

321 **Tabela 1.** Classificação dos modelos experimentais de doença inflamatória intestinal de acordo com a
 322 especificação, para retocolite ulcerativa (RCU) ou doença de Chron (DC). Fonte: Adaptado de Goyal et
 323 al., 2014.

324
 325 O modelo mais utilizado para indução de RCU em roedores utiliza dextran
 326 sulfato de sódio (DSS), um polissacarídeo sulfatado sintético composto de dextrano e
 327 unidade de anidroglicose sulfatada (VAUGHN; MOSS, 2013).

328 Esse modelo foi primeiramente descrito em 1985 no Japão e os primeiros
 329 experimentos foram desenvolvidos em hamsters e posteriormente em camundongos
 330 (OHKUSA, 1985). Por meio deste modelo, pode ser induzida a RCU aguda ou crônica
 331 a depender do peso molecular do DSS, da concentração, da duração e da frequência
 332 de exposição. No entanto, dentro do mesmo modelo, os animais apresentam
 333 susceptibilidade diferente à colite devido a variações genéticas e microbiológicas
 334 (GOYAL et al., 2014).

335 A suplementação da água de roedores com DSS com baixo peso molecular
 336 resulta em características sintomáticas semelhantes à RCU (LAROUÏ et al., 2012). O
 337 DSS carrega uma carga altamente negativa por conta de seus grupos sulfatos, sendo
 338 assim muito tóxico para o epitélio do cólon pois induz erosões que comprometem a
 339 integridade da barreira epitelial, resultando em aumento da permeabilidade epitelial.

340 Além disso, sua propriedade anticoagulante agrava o sangramento intestinal. Por
341 razões desconhecidas, a extensa patologia induzida por DSS está confinada ao
342 intestino grosso, especificamente ao cólon distal, onde há número bastante
343 expressivo de bactérias (CHASSAING et al., 2014).

344 O mecanismo pelo qual o DSS passa pelas células epiteliais da mucosa
345 permanece incerto, mas Laroui *et al.* (2012) sugere o DSS induzir colite em
346 camundongos por meio da formação de nano-lipocomplexos com ácidos graxos de
347 cadeia média no cólon. A especificidade do DSS para o cólon pode decorrer da
348 absorção de água e eletrólitos na presença de numerosas bactérias. Teoricamente, o
349 DSS com carga negativa pode danificar as membranas celulares com carga negativa
350 por forças repulsivas, mas a falta de inflamação induzida por DSS com pesos
351 moleculares inferiores ou superiores argumenta contra isso (CHASSAING et al.,
352 2014).

353 O DSS provoca além de lesões, aumento na permeabilidade intestinal e em
354 análises histoquímicas da distribuição tecidual de DSS com peso molecular de 40 kDa
355 demonstraram que o DSS penetra na membrana mucosa do intestino e um dia após
356 o tratamento com DSS já é possível encontrar pequenas quantidades de DSS em
357 macrófagos no intestino grosso, nos linfonodos mesentéricos e nas células de Kupffer
358 no fígado, com três dias já é possível encontrar o DSS em alguns macrófagos no baço
359 e 7 dias no rim. DSS foi observado nas células de Kupffer do fígado mesmo 8 semanas
360 após a remoção do DSS (KITAJIMA; TAKUMA; MORIMOTO, 1999). Durante a fase
361 crônica da colite por DSS, quantidades consideráveis de DSS também foram
362 encontradas no baço (COOPER et al., 1993). As principais vias de excreção do DSS
363 são a urina e as fezes. Assim, a presença de DSS nas células epiteliais dos túbulos
364 renais proximais após 7 dias de tratamento com DSS é uma indicação do processo
365 de excreção do DSS absorvido (KITAJIMA; TAKUMA; MORIMOTO, 1999).

366 A eficácia da RCU induzida por DSS depende de vários fatores, incluindo peso
367 molecular, 5 kDa para colite leve e 40 kDa para colite grave. A dosagem geralmente
368 é entre 1 e 5%, quando a duração pode ser aguda ou crônica, o modelo pode variar
369 conforme a espécie de roedores também, o C57Bl/6 por exemplo é uma espécie mais
370 susceptível a indução (MELGAR; KARLSSON; MICHAËLSSON, 2005), o sexo dos
371 animais, os machos são mais suscetíveis. A microbiota também apresenta um fator
372 fundamental na indução, em animais livres de microbiota por exemplo, a indução de
373 RCU por DSS não é efetiva (NAGAO-KITAMOTO et al., 2016).

374 Para a indução, o DSS é geralmente administrado por 7 a 10 dias para induzir
375 uma inflamação aguda. Ao prolongar a administração, a RCU aguda pode avançar
376 para a RCU crônica, usualmente administrando-se DSS em ciclos que pode ser de
377 três a cinco, com um período de descanso de uma a duas semanas entre os ciclos
378 (GOYAL et al., 2014).

379 Na fase aguda da RCU causada por DSS podemos observar algumas
380 características clínicas como perda de peso, diarreia, teste de sangue oculto nas fezes
381 positivo, piloereção, anemia e eventualmente, morte, enquanto na fase crônica da
382 colite geralmente não refletem a gravidade da inflamação ou características
383 histológicas encontradas no intestino grosso (PERŠE; CERAR, 2012).

384 Na RCU induzida por DSS, semelhante a RCU que ocorre em humano, há um
385 aumento nos diferentes níveis de citocinas, quimiocinas, óxido nítrico e óxido nítrico
386 sintase indutível (iNOS) que estão implicados na patogênese da DII (GOYAL et al.,
387 2014). O DSS causa colite progressiva e grave com aumento da ativação de NF- κ B,
388 o que piora ainda mais a colite, também ocorre um aumento da expressão de genes
389 de citocinas inflamatórias (IL-1, TNF- α , IL-6 e IL-8) e alguns genes de moléculas de
390 adesão (DOU et al., 2013).

391

392 **2. OBJETIVO**

393

394 *2.1 Objetivo Geral*

395

396 - Avaliar as alterações estruturais e de motilidade do cólon durante o
397 desenvolvimento da retocolite ulcerativa aguda e crônica induzida por DSS em
398 camundongos C57Bl/6.

399

400 *2.2 Objetivos específicos*

401

402 - Padronizar o modelo experimental de RCU aguda e crônica, utilizando exposição
403 ao DSS, no Laboratório de Neurociência Entérica da Universidade Estadual de
404 Londrina.

405

406 - Verificar a evolução de sinais clínicos durante o desenvolvimento da retocolite
407 ulcerativa aguda e crônica induzida por DSS, relacionando com o número de células
408 *tuft*.

409

410 - Caracterizar as alterações anatomopatológicas durante o desenvolvimento da
411 retocolite ulcerativa aguda e crônica induzida por DSS.

412

413 - Avaliar a densidade populacional e morfometria do corpo celular de neurônios
414 mioentéricos gerais, assim como as subpopulações nitrérgica e colinérgica, durante o
415 desenvolvimento da retocolite ulcerativa aguda e crônica induzida por DSS.

416

417 - Elucidar as alterações no padrão de motilidade colônica durante o
418 desenvolvimento da retocolite ulcerativa aguda e crônica induzida por DSS.

419

420 - Relacionar alterações estruturais do plexo mioentérico com variações no padrão
421 de motilidade colônica durante o desenvolvimento da retocolite ulcerativa aguda e
422 crônica induzida por DSS.

423
424
425
426
427
428
429
430
431
432
433
434
435
436
437
438
439
440
441
442
443
444
445
446
447
448
449
450
451
452
453
454
455
456
457
458
459
460
461
462
463
464
465
466

COLONIC MOTILITY ADJUSTMENTS IN ACUTE AND CHRONIC DSS-INDUCED COLITIS

Running Title: Colitis-induced motility changes

Paulo da Silva Watanabe¹; Eduardo José de Almeida Araújo¹.

¹ Department of Histology, State University of Londrina, Londrina, PR, Brazil.

Address for correspondence

Prof. Dr. Eduardo José de Almeida Araújo
Department of Histology, State University of Londrina
Rodovia Celso Garcia Cid PR 445, Km 380, 86051-990, Londrina, PR, Brazil
Tel: +55 (43) 3371 4327
eduardoaraujo@uel.br

Abstract Inflammatory bowel disease is a recurrent inflammation that affects the gastrointestinal tract, causing changes in intestinal motility. The evolution of these changes is not completely understood. The aim of this study was to evaluate the structural and motility changes of the colon during the development of acute and chronic DSS-induced ulcerative colitis (UC) in C57Bl/6 mice. Mice were assigned into 5 groups: control and groups exposed to DSS 3% for 2, 5, 7 days (acute UC) or 3 cycles (chronic UC). Mice were monitored daily. After euthanasia, colon was removed for histological, immunofluorescence and colon motility analysis. There was an increase in the thickness of the mucosa, submucosa, muscle layers and the total wall and reduction in the number of tuft cells. We observed a depletion of goblet cells and an increase in collagen fibers as well as an increase in the positive ChAT myenteric neurons in chronic UC mice. Both UC models caused atrophy of myenteric neurons, reduction in number of colonic contractions, colonic migration motor complex, total time of gastrointestinal transit. Besides, contractions became more vigorous in the ends and longer in the medial region of inflamed colon, especially in chronic UC. We conclude that during the progress of the DSS-induced UC, structural changes occur in the colon, including increase of cholinergic myenteric neurons, followed by variations in the motility pattern of different regions of the colon that taking together characterize colonic dysmotility.

Keywords: dextran sodium sulfate; enteric nervous system; inflammatory bowel; tuft cells; ulcerative colitis.

467
468
469

1 INTRODUCTION

470 Inflammatory bowel disease (IBD) is an idiopathic, chronic and recurrent
471 inflammatory bowel disorder, characterized by abdominal pain and diarrhea ¹. It can
472 result in significant morbidity and mortality, compromising the quality and life
473 expectancy of patients ².

474 IBD occurs worldwide, although it is more common in Western countries.
475 Europe, North America and Oceania are the places with the highest number of
476 diagnosed cases, with incidence rates of 4 to 10 cases per 100,000 inhabitants per
477 year and prevalence rates between 40 to 100 per 100,000 inhabitants, and these
478 numbers are increasing every year ³, which shows us the importance of further
479 studying this disease.

480 There are two major forms of chronic intestinal disorders: Crohn's disease (CD)
481 and ulcerative colitis (UC) ⁴. Some clinical and pathological characteristics of CD and
482 UC are the same, but they also have different characteristics, such as in relation to
483 the regions of gastrointestinal tract that can be affected, as well as in the distribution
484 and depth of inflammation ⁵. CD, unlike UC, can involve any part of the gastrointestinal
485 tract from the oropharynx to the perianal area ⁶. On the other hand, UC is a condition
486 in which the inflammatory response and morphological changes remain confined to
487 the colon and rectum⁷.

488 The aetiology of UC is not yet fully elucidated. There are several factors that can
489 contribute to the pathophysiology of this disease such as imbalance in the tolerance
490 of the innate and adaptive immune system, commensal bacteria, oxidative stress,
491 inflammatory mediators and changes in intestinal permeability ^{3,5}.

492 One of the most used protocols for experimental induction of UC is by using
493 sodium dextran sulfate (DSS) ^{8,9}. The DSS-induced UC is very efficient due the high
494 reproducibility of the lesions mainly in the distal colon, similarly to the UC in humans¹⁰.
495 DSS is a sulphated polysaccharide, heparin like, which has a highly negative charge
496 due to its sulphate groups, being toxic to the colon epithelium inducing erosions that
497 compromise the integrity of the epithelial barrier, resulting in increased epithelial
498 permeability. In addition, its anticoagulant property worsens intestinal bleeding ¹¹.

499 The correlation between inflammation that occurs in the UC and smooth muscle
500 function has been reported in *ex vivo* studies ¹². Since few studies assess *in vivo*

501 information on colonic motility, the studies in the literature are still controversial, some
502 report that UC can cause an increase¹³ or decrease¹⁴ in colonic motility. Studies
503 carried out on animal models usually analyse only a small portion of the colon^{14,15},
504 therefore, the results usually do not reflect the changes that occur in the whole organ.

505 Although there are several studies investigating the pathophysiology of UC^{2,8,9},
506 as its aetiology is still unclear^{3,5}, further studies are needed to evaluate its
507 developments in animal models, investigating the changes caused by this disease in
508 the intestinal epithelium and in the wall of the colon, investigating the acute and chronic
509 model of the disease and also verifying whether these morphological changes
510 interfere with colonic motility. A better understanding of these nuances can point out
511 possible pharmacological targets for treatment of UC.

512 This study aimed to investigate how the development of acute and chronic DSS-
513 induced colitis alters the colonic wall, including myenteric neurons, and how it affects
514 the types of contractions and Colonic Migrating Motor Complex (CMMC) in different
515 portions of the colon in mice.

516

517 **2 Methods**

518

519 *2.1 Ethical approval*

520 The experimental protocols used previously were approved by the Ethics
521 Committee on the Use of Animals (CEUA) of the State University of Londrina (no
522 48/2017)

523 Fifty-five C57BL/6 mice aged 12 weeks (CEMIB/Unicamp) were used during
524 the experiment. The mice were kept in the animal house, in standard polyethylene
525 boxes (29.0 x 18.0 x 12.0 cm) with a metal grid lid, temperature of 22±2°C with
526 exhaustion and alternation of light-dark cycles of 12 hours. All animals receive feed
527 for rodents marketed by NUVITAL® (recommended by the National Research Council
528 and National Health Institute - USA) and liquid *ad libitum*.

529

530 *2.2 Induction to DSS colitis*

531 The animals were distributed into five experimental groups. The control group
532 received only pure autoclaved water and the other groups received water autoclaved

533 supplemented with 3% DSS (Molecular weight: 40000 Da, TdB Consultancy) for
534 different times, as described in Table 1.

535

536 *2.3 Monitoring of clinical signs and number of tufts cells*

537 Throughout the induction, all mice were monitored daily and the loss of body
538 mass, stool consistency and presence of fecal blood was scored to determine the
539 disease activity index (IAD), as previously described by Bento (2011).

540 After the colitis induction, the mice were euthanized by deepening anesthetic
541 with halothane vapor (1%), oxygen (14%) and nitrogen (86%). The total colon was
542 removed, and subsequently processed according as described below for each
543 technique.

544 Aiming immunolabeling tuft cells, colon was divided into two parts, proximal and
545 distal, and then fixed in 4% paraformaldehyde (PFA) for 3 hours at room temperature.
546 Afterwards, it was washed in phosphate-saline buffer (PBS) pH 7.4, 0.1M and kept in
547 saturated sucrose solution (30%) for 24 hours at 4°C, and then frozen in OCT. Two
548 semi-serial 10 µm sections from the proximal region and two from the distal region
549 were performed per mice. Then, the sections were submitted to the
550 immunofluorescence to label the enzyme choline acetyltransferase - ChAT (Table 2).
551 Sections were washed 3 x 5 min in 0.1 M PBS; antigenic block using 2% serum bovine
552 albumin, 10% donkey serum, 0.5% Triton X-100 in PBS 0.1 M pH 7.4; incubation with
553 primary anti-ChAT antibody for 24 hours at room temperature; incubation with
554 secondary antibody (table 2) for 2 hours; slides were then mounted using a coverslip
555 and antifade conjugated with DAPI (INVITROGEN, P36931) and left to dry before
556 viewing under the microscope at 40x. Images of the entire mucosa were captured,
557 where the presence of tuft cells was quantified in each section.

558

559 *2.4 Histopathological analysis*

560 The total length and diameter of the distal colon were measured, in addition, 1
561 cm of the colon was weighed to assess the presence of edema.

562 One-centimeter rings of the colon were collected from all mice and opened by
563 the mesocolic border, fixed in 4% PFA for 3 hours at room temperature. Colons were
564 embedded in paraffin to obtain 4µm semi-serial transversal sections.

565 The sections stained with hematoxylin and eosin (HE) were used for intestinal
566 wall morphometry. Images captured under light microscope at 20x were used to

567 measure the depth of the crypts, thickness of submucosa and muscle layers and total
568 wall. Four images were obtained from each of the four histological sections and, thus,
569 42 measurements were performed per mice using the software Image Pro Plus®¹⁷.

570 For Periodic acid Schiff (PAS) staining, four sections were stained, and six
571 images of each section were captured at 20x. The number of goblet cells present in
572 0.96 mm² of mucosa of each mice was quantified¹⁷.

573 To quantify the collagen, using Sirius Red staining, four sections were stained,
574 24 images were captured per mice, using optical polarization at 40x. The collagen was
575 then quantified by using the software Image Pro Plus®¹⁸. All analyses were performed
576 in a blinded manner.

577

578 *2.5 Morphological evaluation of the myenteric plexus*

579 Colons were fixed in 4% PFA for 3 hours at room temperature and then whole
580 mounts were prepared.

581 Whole mounts were washed in PBS 0.1M pH 7.4 solution and then incubated
582 in antigenic blocking solution and then they were incubated with the primary antibodies
583 shown in table 2. Whole mount preparations were then incubated for 2 h at room
584 temperature with AlexaFluor conjugated secondary antibody (table 2). Then, they
585 were mounted using a coverslip and anti-fade conjugated with DAPI and left to dry
586 before viewing under the microscope at 20x.

587 For neuronal counting, 32 images were captured in the intermediate
588 regions considering the intestinal circumference and all neurons present in these fields
589 were counted. For the morphometric analysis, the area of 100 neuronal body cell per
590 mice was measured using software Image Pro Plus!®. All analyses were performed
591 in a blinded manner.

592

593 *2.6 TGI motility assessment*

594 Gastrointestinal transit was assessed following the method previously
595 described by Welch (2014). A volume of 100 µL of a non-absorbable marker (6%
596 Carmine Red; 0.5% methylcellulose; Sigma-Aldrich, St. Louis, USA) was administered
597 by gavage. Mice were immediately placed in individual cages with free access to food
598 and water. Gastrointestinal transit was expressed as the time between the
599 administration of the biomarker and the appearance of the first red faecal pellet.

600 For the colon manometry we used the experimental procedure similar to
601 described by Fraser (1997). After colitis induction and euthanasia as previously
602 described, the colons were collected and carefully washed and then kept in an organ
603 bath with perfusion of oxygenated Krebs solution at $35^{\circ}\text{C} \pm 1$. Colonic motility was
604 determined by conventional multi-lumen perfusion manometry. Spontaneous
605 contractions were recorded as pressure waves at four points 1 cm apart from each
606 other, taking place in the regions: proximal, medial proximal, medial distal and distal.
607 The recordings were analysed manually using the software Spike2[®].

608

609 *Intracolonic pressure data analysis.*

610 The area under the curve (AUC) of the phasic component of the intraluminal
611 pressure trace for every contraction was analysed. In addition, frequency, amplitude,
612 duration of contractions and duration of quiescence between contractions were
613 determined during 30 min of analysis. Data were obtained from 10 mice from each
614 group.

615 Colonic contractile pressure changes were quantified by measuring the
616 propagation of CMMCs. The propagative nature of contractions was evaluated by
617 determining the direction of appearance of the next peak of the intraluminal pressure
618 wave as described previously²¹. Three different types of propagative and
619 nonpropagative contractions were identified. Contractions that propagate from
620 proximal to distal region were classified as oral-aboral propagating contractions
621 whereas contractions that propagate from distal to proximal were classified as aboral-
622 oral propagating contractions. Lastly, contractions that happen simultaneously at two
623 or more portions of the colon are considered as static.

624 The speed of propagation in mm/s was obtained by dividing the distance
625 between the first (proximal) and the last (distal) pressure sensors (40mm) by the time
626 (s) elapsed between the peaks of the contractions at proximal and distal sites.

627 The amplitude and duration of the contractions were also categorized and
628 quantified according to the number of events that occurred, as previously
629 demonstrated by Gourcerol (2009).

630

631 *2.7 Statistical analysis*

632 Statistical tests were performed using Graphpad Prism[®] 7 software. The data
633 distribution was checked using D'Agostino-Pearson normality test. As all data
634 presented normal distribution, groups were compared using one-way analysis of
635 variance (ANOVA) and Tukey's multiple comparison test. The level of significance was
636 5%.

637

638 **3 RESULTS**

639

640 *Experimental acute and chronic colitis was successfully induced by DSS*

641 Clinical signs of DSS-induced colitis were observed after the third day by means
642 of piloerection, prostration, progressive body weight loss (Fig. 1A), diarrhea and
643 bleeding from 5th day, which contributed for DAI reached values much greater in colitis
644 mice vs control (Fig. 1B) from the 7th day of exposure to DSS ($P < 0.05$). Edema was
645 observed only in DSS 3C group ($P < 0.05$; Fig. 1C). In addition, we observed the typical
646 shortening of colon size in colitis mice ($P < 0.05$; Figs. 1D and E). Based on these
647 results, DSS7d group was considered the representative for acute UC and the DSS3C
648 group for chronic UC during the next experiments.

649 The histopathological analysis showed an architectural irregularity in the crypts,
650 a massive leukocyte infiltrate in the submucosa and lamina propria, irregular epithelial
651 surface, rupture of the intestinal epithelium and presence of inflammatory cells
652 infiltrated in myenteric plexus ganglia of the colitis groups vs control (fig 2A-E). The
653 leukocyte infiltrate caused an increase in the thickness of the colonic mucosa and total
654 wall for all groups, and submucosa, circular muscle and total muscle of the DSS3C
655 groups ($P < 0.05$; Fig. 2F). Goblet cells were depleted only in DSS3C group ($P < 0.05$;
656 Fig. 2G-J). Fibrosis was observed in both colitis groups characterized by the
657 increasing in the quantity of collagen types I and III ($P < 0.05$; Fig. 2L and M). In
658 addition, we observed that the number of tuft cells in the total colon decreased
659 progressively during the course of the disease ($P < 0.05$; Fig. 3A), reflected by the
660 impact of DSS-induced colitis on the proximal colon rather than distal colon (Fig. 3B
661 and C).

662

663 *DSS-induced colitis promoted atrophy of myenteric neurons and increase in the*
664 *number of cholinergic neurons*

665 The number of general myenteric neurons (PGP9.5⁺) did not change between
666 the experimental groups (Fig. 4A) but these cells were atrophied in both UC groups
667 (DSS7d and DSS3C) when compared to the control group ($P < 0.05$; fig 4B). Similar
668 result was observed for the nitrergic neurons (nNOS⁺), however the atrophy was
669 observed only in the DSS7d group ($P < 0.05$; Fig 4B). Contrarily, the number of
670 cholinergic neurons (ChAT⁺) increased in the DSS3C group ($P < 0.05$; Fig. 4A), which
671 provoked a significant increase in the ratio of ChAT/PGP9.5 myenteric neurons ($P <$
672 0.05 ; Fig. 4D). However, cholinergic neurons were also atrophied as also observed for
673 the other types of myenteric neurons ($P < 0.05$; Fig. 4B). All these results are illustrated
674 on the Fig. 5.

675

676 *Colonic motility adjustments during course of colitis*

677 Chronic DSS-induced UC caused increase in the area under the curve (AUC)
678 of contractions in almost the entire colon and, on the other hand, acute colitis provoked
679 reduction only in the middle distal portion ($P < 0.05$; Fig. 6A). Chronic UC caused
680 increase in the contraction amplitude of the proximal and distal colon, where it was
681 observed reduction of the number of contractions < 25 mmHg ($P < 0.05$; Figs. 6B-C).
682 Regarding the number of overall contractions, it has reduced progressively over the
683 entire colon during the course of the disease, but significant changes were observed
684 only in the chronic phase (Figs. 6C-F).

685 Although the proportion of time that the colon has kept in contraction during the
686 manometric observation (30 min) was not changed in almost its whole extension (Fig.
687 7B), the duration of the contractions increased in the middle portion of the colon of
688 chronic UC mice ($P < 0.05$; Fig. 7A). On the other hand, the duration of colonic
689 contractions in acute UC mice was not changed (Fig. 7A), but the proportion of
690 contraction tended to reduce in the entire organ, becoming significant in the distal
691 region ($P < 0.05$; Fig. 7B). The relaxation time between contractions (Fig. 7C) and the
692 proportion of quiescence time (Fig. 7D) was unchanged in both UC groups. Besides,
693 we observed fewer contractions lasting less than < 100 seconds in the entire colon in
694 both UC groups and greater number of contractions lasting between 100 and 150
695 seconds in the middle distal colon of chronic UC mice ($P < 0.05$; Figs. 7E-H).

696 All these adjustments implied in changes on CMMCs. Acute and chronic DSS
697 induced-colitis caused reduction in the number and increase in the duration of CMMCs
698 ($P < 0.05$; Figs. 8A and B), but no changing the interval of time between CMMCs was

699 observed (Fig. 8C). The speed propagation was reduced and time of gastrointestinal
700 transit was slower in UC mice when compared to control group ($P < 0.05$; Figs. 8D
701 and E). The number of aboral-oral and static contractions did not change, but the
702 frequency of oral-aboral contractions was reduced in both UC groups ($P < 0.05$; Figs.
703 8E and F).

704

705 **4. DISCUSSION**

706

707 The incidence of IBD is progressively growing in many countries, however there
708 are many aspects of the disease that remain unclear. Among the several experimental
709 models developed in order to research aetiology, pathophysiology and treatment of
710 the IBD, the DSS-induced experimental colitis is one of the mostly used in the world
711 ²³. Independently of the model, there are consistent evidences of IBD alters colonic
712 motility, however we do not understand yet how DSS-induced colitis impacts the
713 manometric parameters of contractions in different portions of the colon.

714 In this report, we showed that acute and chronic DSS-induced colitis
715 experimental models imply in different adjustments of colonic motility. Although the
716 typical inflammatory parameters were noticed in the acute colitis model, salient
717 changes were not observed on the colonic motility during the first week of exposition
718 to DSS. However, after three cycles of exposition, the colon was less mobile and
719 slower especially in its middle portion in spite of the contractions on the proximal and
720 distal ends were more vigorous.

721 It is known that DSS causes a toxic effect directly to the colonic epithelium
722 provoking intestinal morphophysiological changes similar to several
723 pathophysiological aspects of UC, characterized by shortening of the colon, bloody
724 diarrhoea and loss of sustained body mass ¹⁸ exactly as we observed in our study.
725 Besides, the typical histopathology observed in UC ^{2,11} such as goblet cell depletion,
726 epithelial degeneration and necrosis, inflammatory cell infiltration in the lamina propria
727 and submucosa were also noticed in mice acutely and chronically exposed to DSS.

728 The colonic epithelial rupture is the pitch to trigger the inflammatory process ²⁴,
729 which make the intestinal barrier crucial to prevent UC. Recently, some researches
730 highlighted the role of tuft cells as important modulators of the integrity of the intestinal
731 mucosa ^{25,26} and others showed DSS-induced structural changes were more severe
732 when the number of tuft cells is reduced ^{25,27}. In this study we showed that tuft cells

733 did not reduce right after the exposition to DSS. It was necessary at least five days of
734 exposition to observe reduction in the number of tuft cells. Besides, the proximal colon
735 showed more susceptible to deplete tuft cells in comparison to distal colon, which is
736 on the opposite way to the description of DSS affects more the distal colon in
737 comparison to the proximal region ¹¹. Thus, our results indicate that the number of tuft
738 cells is not altered directly by the exposition to DSS but it is a consequence of the Th1
739 response usually observed in DSS-induced colitis in C57BL6 ^{11,28}.

740 During the DSS-induced immune response, many cells migrate to the colonic
741 wall especially to the mucosa and submucosa ⁸. Besides, it is very common to report
742 proctitis in UC, which consists of an inflammatory infiltrate within the submucosal or
743 myenteric plexus ²⁹. This inflammatory environment certainly contributed to modulate
744 myenteric neurons and colonic motility as we discussed below.

745 The structure and neurochemical composition of the SNE are usually altered
746 during active IBD. The number of mucosal and muscular nerve fibers increases,
747 together with the immunoreactivity of neurochemicals, including tyrosine hydroxylase,
748 substance P, peptide related to the calcitonin peptide, vasoactive intestinal
749 polypeptide, 5-hydroxytryptamine and nitric oxide ³⁰. Hypertrophy and hyperplasia of
750 nerve fibers and architectural changes in neuronal cell bodies and enteric glial cells
751 are usually found in colitis tissue ^{31,32}

752 The severity of intestinal inflammation is associated with the density of enteric
753 innervation. Thus, enteric neurons are likely to be able to influence and to be
754 influenced by the severity of inflammation by releasing neurotransmitters /
755 neuromodulators. Inflammation is more severe when the ENS is hyperplastic and less
756 severe when the ENS is hypoplastic ³³.

757 Although it is suggested that the inflammation observed in UC patients is
758 restricted to colonic mucosa ⁵, some studies indicate that changes in myenteric
759 neurons can happen ^{32,34}, but there are several controversies. There are findings
760 showing increase in the number of neurons, suggestive of neurogenesis ³⁵, however
761 in some cases there is no change or decrease in the number of myenteric neurons ³⁶.

762 In DSS-induced colitis, it was observed that the quantity of ChAT in the colon
763 was higher compared to the control group, but not reflecting on increase in the amount
764 of ChAT⁺ neuronal bodies ³⁴. Changes in the neuronal chemical code, such as the
765 increase in the number of ChAT⁺ neurons observed in our study, are considered as
766 mechanism of adaptation to stimuli ³⁷. Thereby, it may be related to a possible

767 mechanism of adaptation in order to normalize the pattern of colonic contractions in
768 response to the inflammatory environment. It could help to explain the general
769 reduction in the number of contractions (probably involving increased interneuronal
770 activity) and the increase of strength of contractions (probably involving increased
771 excitatory motor neuronal activity) in the colonic ends of DSS-induced colitis mice. Our
772 results support the involvement of interneuronal activity as we will explain below.

773 DSS-induced colitis can upregulate the expression of ChAT which has the
774 potential to increase rhythmic phasic contractions ³⁴. On the other hand, the DSS-
775 induced inflammation inhibits the reactivity of smooth muscle to ACh resulting into
776 two opposite changes which suppress the rhythmic phasic contractions in DSS
777 inflammation ^{38,39}.

778 During intestinal inflammatory processes, dysmotility may occur depending on
779 the experimental model used ⁴⁰. Colonic motility has been shown to decrease during
780 chemically induced colitis ⁴¹, an effect attributed to the suppression of excitatory and
781 inhibitory signalling in the colon ³⁴ and loss of myenteric neurons ³⁶. However, the
782 impact of DSS-induced colitis on profile of contractions and CMMC activity remain to
783 be definitively determined.

784 Considering only the DSS-induced colitis model, the intestinal immune
785 response can be different depending on the specie, strain and gender of the
786 experimental animal ²³. Here, we have chosen to use male C57Bl/6 mice because
787 they show an immune response more intense ²⁸. This type of immune response
788 causes hypocontractability, reduced motility ⁴² and we showed these alterations on
789 colonic motility are progressive during the exposition to DSS. After three weeks,
790 contractions were stronger in the colonic ends due reduction in the number of less
791 strength contractions. Besides, they have become longer in the middle region due
792 reduction in the number of short duration contractions. For these reasons, the number
793 of overall contractions was reduced in the chronic DSS-induced colitis. Interestingly, it
794 would be expected to observe a greater number of contraction when we consider that
795 the proportion of cholinergic neurons was increased in the inflamed colon. This
796 contradiction indicates that the extended number of cholinergic neurons plays as
797 interneurons in order to coordinate the movements of the inflamed colon.

798 Our results demonstrate that reduction in the number of contractions reflected
799 on the reduced number of CMMCs, especially in oral-aboral direction, in DSS-induced
800 colitis. Similarly, the increase in the duration of contractions also impacted the duration

801 of CMMCs once they became double longer in colitis mice with chronic inflammation.
802 This dysmotility may have contributed to the development of diarrhea in colitis mice,
803 but it is important to consider that this clinical sign can be also related to bleeding,
804 deficiency in the absorption of water and electrolytes and efflux of fluids promoted by
805 inflammation ⁴³.

806 Considering other chemically induced colitis models, it was showed less
807 CMMCs and lower amplitude of contractions in TNBS-induced UC, but the duration of
808 contractions was also increased ¹⁴. TNBS also demonstrated that the speed of
809 propulsive motility was slower in inflamed colon ⁴⁴ being completely obstructed or
810 temporarily interrupted ^{41,45}. Unfortunately, there are no other manometric studies
811 evaluating the whole colon in animals exposed to colitis-inducing chemical agents.

812 Few information is available regarding the mechanisms involved in adjustments
813 of colonic motility triggered by inflammation. The inhibition of CMMC in TNBS-induced
814 UC is not due direct effects of IL-1B (Hofma et al., 2018). Studies suggest the
815 increased prostaglandin synthesis due upregulation of cyclooxygenase 2 in myenteric
816 neurons during UC may contribute to the reduction in colonic motility ⁴⁶. Other suggest
817 that about 50% of primary afferent neurons, or interneurons, exhibit spontaneous
818 action potentials in the colonic inflamed regions. This can promote the activation of
819 upward and downward contracting inhibitory signals. This uncontrolled neuronal
820 behaviour can result in mixed excitatory and inhibitory messages converging on
821 smooth muscle throughout the inflamed region causing a kind of intestinal fibrillation
822 ⁴⁷.

823 We concluded DSS was efficient to induce acute and chronic colitis, causing
824 increasing in the number of cholinergic neurons and also progressive dysmotility
825 pattern during the progress of the disease. In acute DSS-induced colitis the colonic
826 motility was little changed, but during the choric colitis the colon has become less
827 mobile and slower in its middle portion and stronger on its proximal and distal ends.

828

829 **ACKNOWLEDGMENT**

830 This study was financed in part by the Coordenação de Aperfeiçoamento de Pessoal
831 de Nível Superior – Brasil (CAPES) – Finance Code 001

832

833

834 **REFERENCES**

835 1. Ordás I, Eckmann L, Talamini M, Baumgart DC, Sandborn WJ. Ulcerative

- 836 colitis. *Lancet*. 2012;380(9853):1606-1619. doi:10.1016/S0140-
837 6736(12)60150-0
- 838 2. Laroui H, Ingersoll SA, Liu HC, et al. Dextran Sodium Sulfate (DSS) Induces
839 Colitis in Mice by Forming Nano-Lipocomplexes with Medium-Chain-Length
840 Fatty Acids in the Colon. Niess J-H, ed. *PLoS One*. 2012;7(3):e32084.
841 doi:10.1371/journal.pone.0032084
- 842 3. Alatab S, Sepanlou SG, Ikuta K, et al. The global, regional, and national
843 burden of inflammatory bowel disease in 195 countries and territories, 1990–
844 2017: a systematic analysis for the Global Burden of Disease Study 2017.
845 *Lancet Gastroenterol Hepatol*. 2020;5(1):17-30. doi:10.1016/S2468-
846 1253(19)30333-4
- 847 4. Cury D, Oliveira R, Cury M. Inflammatory bowel diseases: time of diagnosis,
848 environmental factors, clinical course, and management – a follow-up study in
849 a private inflammatory bowel disease center (2003–2017). *J Inflamm Res*.
850 2019;Volume 12:127-135. doi:10.2147/JIR.S190929
- 851 5. Goyal N, Rana A, Ahlawat A, Bijjem KR V., Kumar P. Animal models of
852 inflammatory bowel disease: a review. *Inflammopharmacology*.
853 2014;22(4):219-233. doi:10.1007/s10787-014-0207-y
- 854 6. Hendrickson BA, Gokhale R, Cho JH. Clinical Aspects and Pathophysiology of
855 Inflammatory Bowel Disease. *Clin Microbiol Rev*. 2002;15(1):79-94.
856 doi:10.1128/CMR.15.1.79-94.2002
- 857 7. Baumgart DC, Sandborn WJ. Inflammatory bowel disease: clinical aspects and
858 established and evolving therapies. *Lancet*. 2007;369(9573):1641-1657.
859 doi:10.1016/S0140-6736(07)60751-X
- 860 8. Perše M, Cerar A. Dextran Sodium Sulphate Colitis Mouse Model: Traps and
861 Tricks. *J Biomed Biotechnol*. 2012;2012:1-13. doi:10.1155/2012/718617
- 862 9. Hartog A, Belle FN, Bastiaans J, et al. A potential role for regulatory T-cells in
863 the amelioration of DSS induced colitis by dietary non-digestible
864 polysaccharides. *J Nutr Biochem*. 2015;26(3):227-233.
865 doi:10.1016/j.jnutbio.2014.10.011
- 866 10. Randhawa PK, Singh K, Singh N, Jaggi AS. A review on chemical-induced
867 inflammatory bowel disease models in rodents. *Korean J Physiol Pharmacol*.
868 2014;18(4):279-288. doi:10.4196/kjpp.2014.18.4.279
- 869 11. Chassaing B, Aitken JD, Malleshappa M, Vijay-Kumar M. Dextran Sulfate

- 870 Sodium (DSS)-Induced Colitis in Mice. *Curr Protoc Immunol*. 2014;104(1):612-
871 615. doi:10.1002/0471142735.im1525s104
- 872 12. kiyosue m., Fujisawa M, Kinoshita K, Hori M, Ozaki H. Different
873 susceptibilities of spontaneous rhythmicity and myogenic contractility to
874 intestinal muscularis inflammation in the hapten-induced colitis.
875 *Neurogastroenterol Motil*. 2006;18(11):1019-1030. doi:10.1111/j.1365-
876 2982.2006.00841.x
- 877 13. Bassotti G, de Roberto G, Chistolini F, Sietchiping-Nzepa F, Morelli O, Morelli
878 A. Twenty-four-hour manometric study of colonic propulsive activity in patients
879 with diarrhea due to inflammatory (ulcerative colitis) and non-inflammatory
880 (irritable bowel syndrome) conditions. *Int J Colorectal Dis*. 2004;19(5):493-497.
881 doi:10.1007/s00384-004-0604-6
- 882 14. Hofma BR, Wardill HR, Mavrangelos C, et al. Colonic migrating motor
883 complexes are inhibited in acute tri-nitro benzene sulphonic acid colitis. Shi X-
884 Z, ed. *PLoS One*. 2018;13(6):e0199394. doi:10.1371/journal.pone.0199394
- 885 15. Calabresi MFF, Tanimoto A, Próspero AG, et al. Changes in colonic
886 contractility in response to inflammatory bowel disease: Long-term assessment
887 in a model of TNBS-induced inflammation in rats. *Life Sci*.
888 2019;236(10):116833. doi:10.1016/j.lfs.2019.116833
- 889 16. Bento AF, Claudino RF, Dutra RC, Marcon R, Calixto JB. Omega-3 Fatty Acid-
890 Derived Mediators 17(R)-Hydroxy Docosahexaenoic Acid, Aspirin-Triggered
891 Resolvin D1 and Resolvin D2 Prevent Experimental Colitis in Mice. *J Immunol*.
892 2011;187(4):1957-1969. doi:10.4049/jimmunol.1101305
- 893 17. Trevizan AR, Vicentino-Vieira SL, da Silva Watanabe P, et al. Kinetics of acute
894 infection with *Toxoplasma gondii* and histopathological changes in the
895 duodenum of rats. *Exp Parasitol*. 2016;165:22-29.
896 doi:10.1016/j.exppara.2016.03.015
- 897 18. Maria-Ferreira D, Nascimento AM, Cipriani TR, et al. Rhamnogalacturonan, a
898 chemically-defined polysaccharide, improves intestinal barrier function in DSS-
899 induced colitis in mice and human Caco-2 cells. *Sci Rep*. 2018;8(1):12261.
900 doi:10.1038/s41598-018-30526-2
- 901 19. Welch MG, Margolis KG, Li Z, Gershon MD. Oxytocin regulates
902 gastrointestinal motility, inflammation, macromolecular permeability, and
903 mucosal maintenance in mice. *Am J Physiol Liver Physiol*. 2014;307(8):G848-

- 904 G862. doi:10.1152/ajpgi.00176.2014
- 905 20. Fraser R, Frisby C, Schirmer M, et al. Effects of fractionated abdominal
906 irradiation on small intestinal motility--studies in a novel in vitro animal model.
907 *Acta Oncol.* 1997;36(7):705-710.
908 <http://www.ncbi.nlm.nih.gov/pubmed/9490087>
- 909 21. Powell AK, Fida R, Bywater RAR. Motility in the isolated mouse colon:
910 migrating motor complexes, myoelectric complexes and pressure waves.
911 *Neurogastroenterol Motil.* 2003;15(3):257-266. doi:10.1046/j.1365-
912 2982.2003.00412.x
- 913 22. Gourcerol G, Wang L, Adelson DW, Larauche M, Taché Y, Million M.
914 Cholinergic giant migrating contractions in conscious mouse colon assessed
915 by using a novel noninvasive solid-state manometry method: modulation by
916 stressors. *Am J Physiol Liver Physiol.* 2009;296(5):G992-G1002.
917 doi:10.1152/ajpgi.90436.2008
- 918 23. Eichele DD, Kharbanda KK. Dextran sodium sulfate colitis murine model: An
919 indispensable tool for advancing our understanding of inflammatory bowel
920 diseases pathogenesis. *World J Gastroenterol.* 2017;23(33):6016-6029.
921 doi:10.3748/wjg.v23.i33.6016
- 922 24. Gitter AH, Wullstein F, Fromm M, Schulzke JD. Epithelial barrier defects in
923 ulcerative colitis: Characterization and quantification by electrophysiological
924 imaging. *Gastroenterology.* 2001;121(6):1320-1328.
925 doi:10.1053/gast.2001.29694
- 926 25. Yi J, Bergstrom K, Fu J, et al. Dclk1 in tuft cells promotes inflammation-driven
927 epithelial restitution and mitigates chronic colitis. *Cell Death Differ.*
928 2019;26(9):1656-1669. doi:10.1038/s41418-018-0237-x
- 929 26. Banerjee A, McKinley ET, von Moltke J, Coffey RJ, Lau KS. Interpreting
930 heterogeneity in intestinal tuft cell structure and function. *J Clin Invest.*
931 2018;128(5):1711-1719. doi:10.1172/JCI120330
- 932 27. Qu D, Weygant N, May R, et al. Ablation of Doublecortin-Like Kinase 1 in the
933 Colonic Epithelium Exacerbates Dextran Sulfate Sodium-Induced Colitis.
934 Heimesaat MM, ed. *PLoS One.* 2015;10(8):e0134212.
935 doi:10.1371/journal.pone.0134212
- 936 28. Acharya S, Timilshina M, Jiang L, et al. Amelioration of Experimental
937 autoimmune encephalomyelitis and DSS induced colitis by NTG-A-009

- 938 through the inhibition of Th1 and Th17 cells differentiation. *Sci Rep.*
939 2018;8(1):7799. doi:10.1038/s41598-018-26088-y
- 940 29. Lee CMY, Kumar RK, Lubowski DZ, Burcher E. Neuropeptides and nerve
941 growth in inflammatory bowel diseases: a quantitative immunohistochemical
942 study. *Dig Dis Sci.* 2002;47(3):495-502. doi:10.1023/a:1017943430627
- 943 30. Brierley SM, Linden DR. Neuroplasticity and dysfunction after gastrointestinal
944 inflammation. *Nat Rev Gastroenterol Hepatol.* 2014;11(10):611-627.
945 doi:10.1038/nrgastro.2014.103
- 946 31. Geboes K, Collins S. Structural abnormalities of the nervous system in Crohn's
947 disease and ulcerative colitis. *Neurogastroenterol Motil.* 1998;10(3):189-202.
948 doi:10.1046/j.1365-2982.1998.00102.x
- 949 32. Belkind-Gerson J, Graham HK, Reynolds J, et al. Colitis promotes neuronal
950 differentiation of Sox2+ and PLP1+ enteric cells. *Sci Rep.* 2017;7(1):2525.
951 doi:10.1038/s41598-017-02890-y
- 952 33. Margolis KG, Stevanovic K, Karamooz N, et al. Enteric Neuronal Density
953 Contributes to the Severity of Intestinal Inflammation. *Gastroenterology.*
954 2011;141(2):588-598.e2. doi:10.1053/j.gastro.2011.04.047
- 955 34. Winston JH, Li Q, Sarna SK. Paradoxical regulation of ChAT and nNOS
956 expression in animal models of Crohn's colitis and ulcerative colitis. *Am J*
957 *Physiol Liver Physiol.* 2013;305(4):G295-G302. doi:10.1152/ajpgi.00052.2013
- 958 35. Belkind-Gerson J, Hotta R, Nagy N, et al. Colitis Induces Enteric Neurogenesis
959 Through a 5-HT4-dependent Mechanism. *Inflamm Bowel Dis.* 2015;21(4):870-
960 878. doi:10.1097/MIB.0000000000000326
- 961 36. Gulbransen BD, Bashashati M, Hirota SA, et al. Activation of neuronal P2X7
962 receptor-pannexin-1 mediates death of enteric neurons during colitis. *Nat*
963 *Med.* 2012;18(4):600-604. doi:10.1038/nm.2679
- 964 37. Makowska K, Gonkowski S. The Influence of Inflammation and Nerve Damage
965 on the Neurochemical Characterization of Calcitonin Gene-Related Peptide-
966 Like Immunoreactive (CGRP-LI) Neurons in the Enteric Nervous System of the
967 Porcine Descending Colon. *Int J Mol Sci.* 2018;19(2):548.
968 doi:10.3390/ijms19020548
- 969 38. D'Autréaux F, Margolis KG, Roberts J, et al. Expression Level of Hand2
970 Affects Specification of Enteric Neurons and Gastrointestinal Function in Mice.
971 *Gastroenterology.* 2011;141(2):576-587.e6. doi:10.1053/j.gastro.2011.04.059

- 972 39. Shi X-Z, Winston JH, Sarna SK. Differential immune and genetic responses in
973 rat models of Crohn's colitis and ulcerative colitis. *Am J Physiol Liver Physiol.*
974 2011;300(1):G41-G51. doi:10.1152/ajpgi.00358.2010
- 975 40. Shea-Donohue T, Notari L, Sun R, Zhao A. Mechanisms of smooth muscle
976 responses to inflammation. *Neurogastroenterol Motil.* 2012;24(9):802-811.
977 doi:10.1111/j.1365-2982.2012.01986.x
- 978 41. Hoffman JM, McKnight ND, Sharkey KA, Mawe GM. The relationship between
979 inflammation-induced neuronal excitability and disrupted motor activity in the
980 guinea pig distal colon. *Neurogastroenterol Motil.* 2011;23(7):673-e279.
981 doi:10.1111/j.1365-2982.2011.01702.x
- 982 42. Moreels TG, De Man JG, De Winter BY, Timmermans J-P, Herman AG,
983 Pelckmans PA. Effect of 2,4,6-trinitrobenzenesulphonic acid (TNBS)-induced
984 ileitis on the motor function of non-inflamed rat gastric fundus.
985 *Neurogastroenterol Motil.* 2001;13(4):339-352. doi:10.1046/j.1365-
986 2982.2001.00273.x
- 987 43. Barros LL, Farias AQ, Rezaie A. Gastrointestinal motility and absorptive
988 disorders in patients with inflammatory bowel diseases: Prevalence, diagnosis
989 and treatment. *World J Gastroenterol.* 2019;25(31):4414-4426.
990 doi:10.3748/wjg.v25.i31.4414
- 991 44. Linden DR, Chen J-X, Gershon MD, Sharkey KA, Mawe GM. Serotonin
992 availability is increased in mucosa of guinea pigs with TNBS-induced colitis.
993 *Am J Physiol Liver Physiol.* 2003;285(1):G207-G216.
994 doi:10.1152/ajpgi.00488.2002
- 995 45. Strong DS, Cornbrooks CF, Roberts JA, Hoffman JM, Sharkey KA, Mawe GM.
996 Purinergic neuromuscular transmission is selectively attenuated in ulcerated
997 regions of inflamed guinea pig distal colon. *J Physiol.* 2010;588(5):847-859.
998 doi:10.1113/jphysiol.2009.185082
- 999 46. Roberts PJ. Neuronal COX-2 expression in human myenteric plexus in active
1000 inflammatory bowel disease. *Gut.* 2001;48(4):468-472.
1001 doi:10.1136/gut.48.4.468
- 1002 47. Mawe GM. Colitis-induced neuroplasticity disrupts motility in the inflamed and
1003 post-inflamed colon. *J Clin Invest.* 2015;125(3):949-955. doi:10.1172/JCI76306
1004
1005

1006

1007 **TABLES**

1008

1009 **Table 1.** Organization of groups to induce UC with DSS in drinking water.

Groups	Treatment
Control (GC)	Pure water for 7 days
DSS 2 Days (DSS2d)	DSS 3% for 2 consecutive days
DSS 5 Days (DSS5d)	DSS 3% for 5 consecutive days
DSS 7 Days (DSS7d)	DSS 3% for 7 consecutive days
Chronic (DSS3C)	Three cycles of DSS 3% for 5 days alternated with 7 days of pure water.

1010

1011

1012

1013 **Table 2.** Primary and secondary antibodies used for the immunofluorescence technique.

ANTIBODY	SPECIES	DILUTION	MANUFACTURER	CODE
anti-PGP9.5	Rabbit	1:500	Abcam	AB27053
anti-nNOS	Goat	1:300	Abcam	AB1376
anti-ChAT	Goat	1:100	Merck	AB144P
Alexa Fluor® 488 anti-rabbit	Donkey	1:500	Invitrogen	A-21206
Alexa Fluor® 568 Anti-goat	Donkey	1:500	Invitrogen	A-11057

1014

1015 FIGURES AND LEGENDS

1016

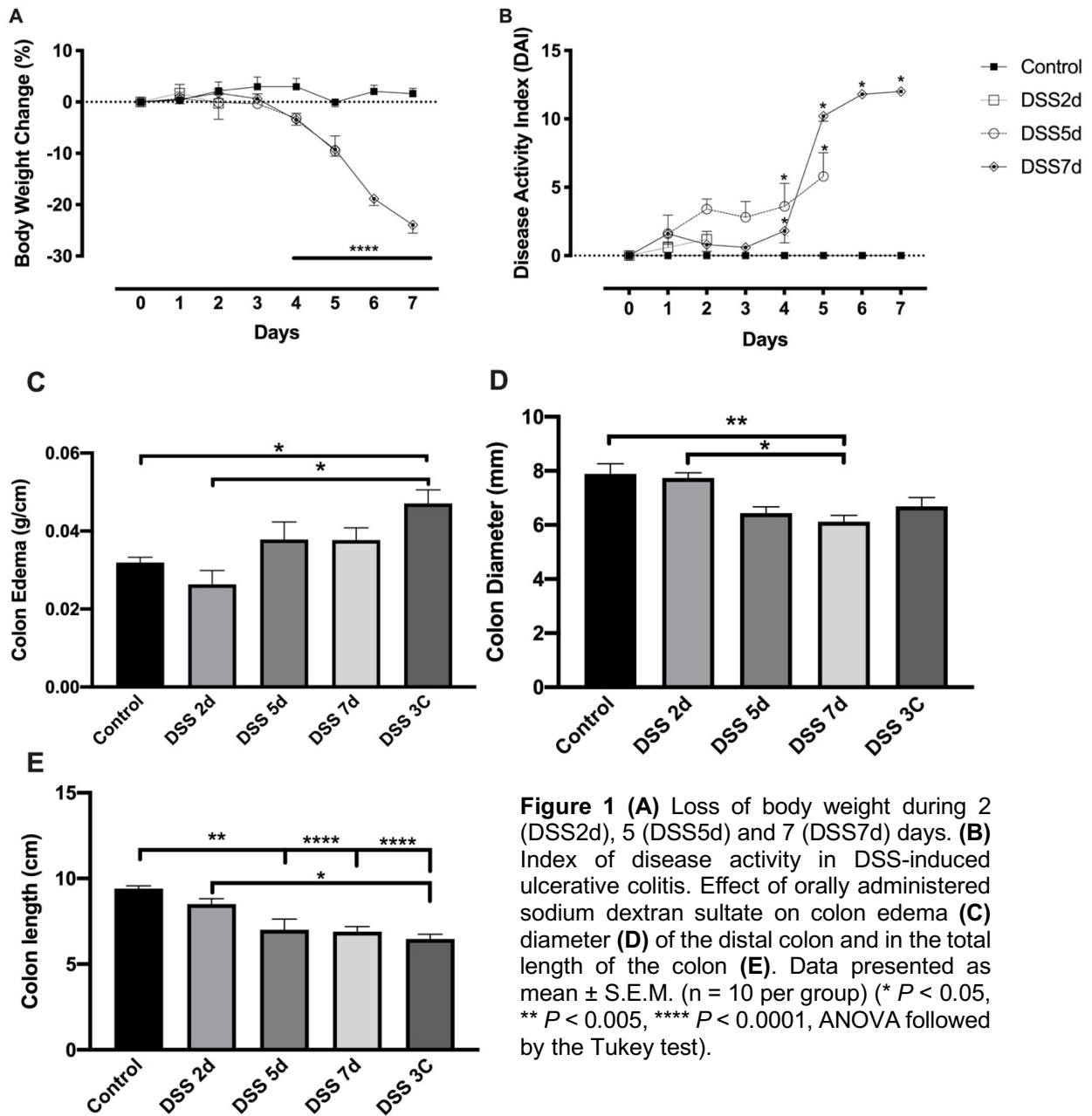


Figure 1 (A) Loss of body weight during 2 (DSS2d), 5 (DSS5d) and 7 (DSS7d) days. (B) Index of disease activity in DSS-induced ulcerative colitis. Effect of orally administered sodium dextran sulfate on colon edema (C) diameter (D) of the distal colon and in the total length of the colon (E). Data presented as mean \pm S.E.M. ($n = 10$ per group) (* $P < 0.05$, ** $P < 0.005$, **** $P < 0.0001$, ANOVA followed by the Tukey test).

1017

1018

1019

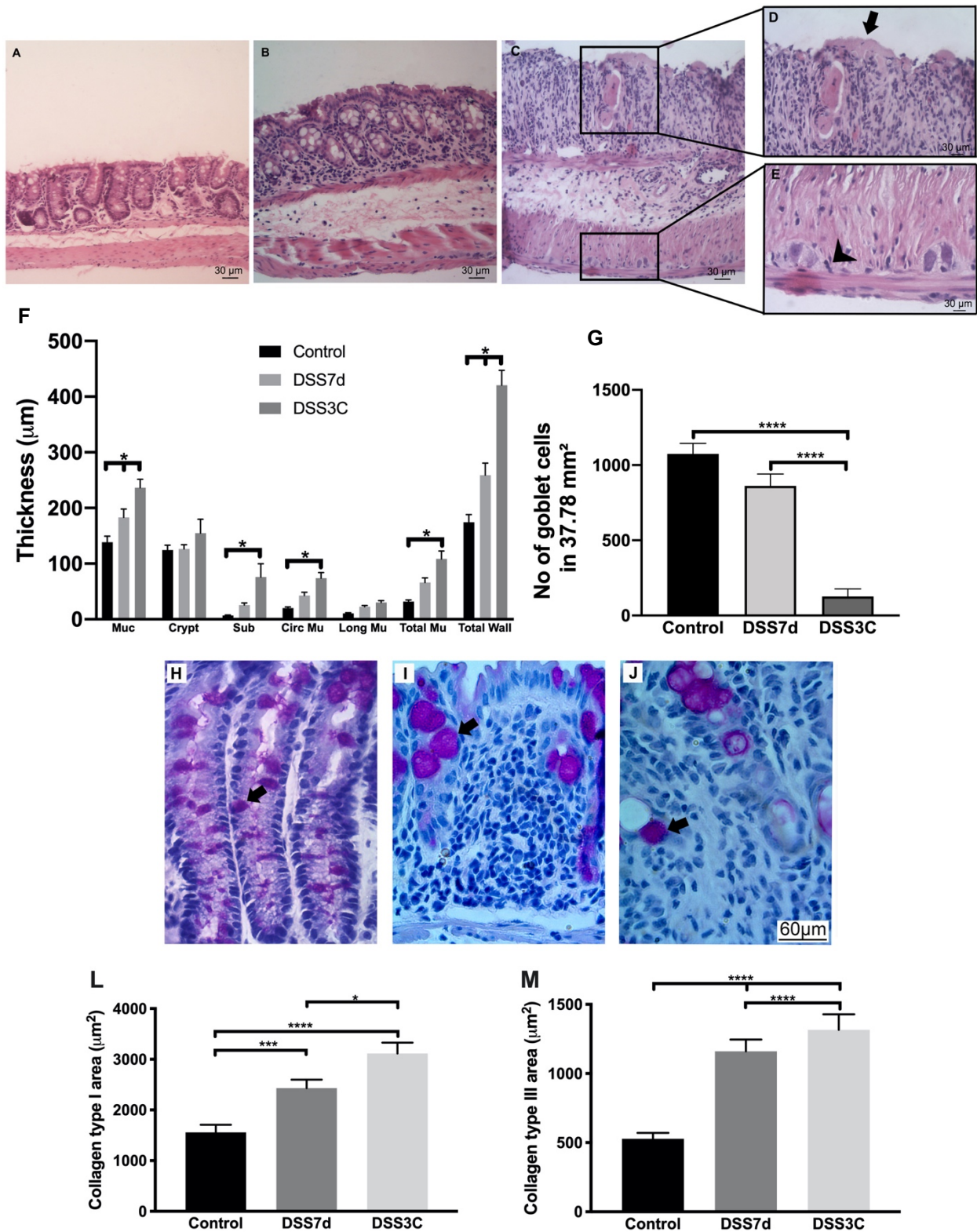


Figure 5 Photomicrograph of histological sections stained by H&E. Groups: Control (**A**) DSS7d (**B**) and DSS3C (**C**). (**D**) The arrow shows a rupture of the intestinal epithelium. (**E**) arrowhead - Inflammatory infiltrate within the ganglion. (**F**) Graph representing the distal colon's analysis of wall. Mucosa thickness (Muc), crypt depth (crypt), submucosa (sub), circular muscle (Circ. Mu.), Longitudinal muscle (Long. Mu.), Total muscle (Total Mu.) were analyzed. Histological sections of the distal colon stained with PAS from mice in the control group (**H**) and exposed to the DSS for 7 (DSS7d) days (**I**) and the group with chronic colitis (DSS3C) (**J**) and in (**G**) Graph representative. Arrow points to goblet cells. Type I (**L**) and III (**M**) collagen quantification using Sirius Red staining. Data presented as mean \pm S.E.M. ($n = 5$ per group) (* $P < 0.05$, *** $P < 0.005$, **** $P < 0.0001$, ANOVA followed by the Tukey test).

1020
1021

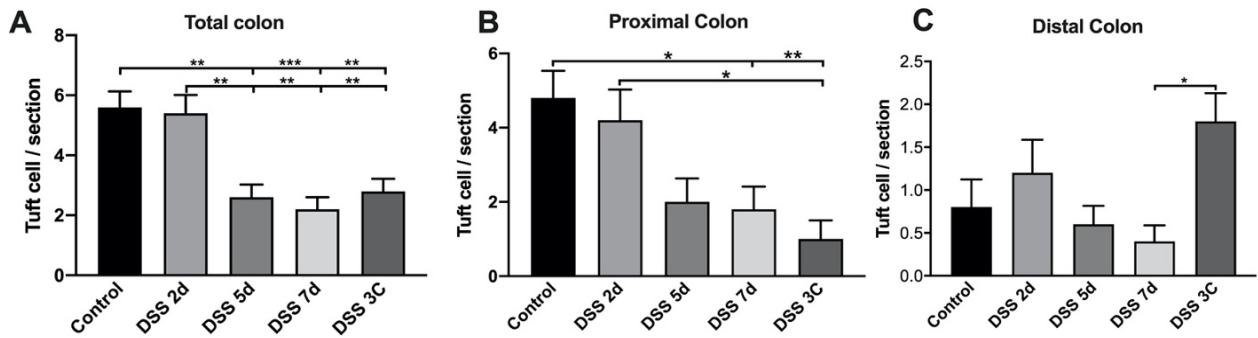


Figure 6 (A) Number of tuft cells in mice's total colon exposed to DSS for 2 (DSS2d), 5 (DSS5d), 7 (DSS7d) days and also in the group induced to chronic ulcerative colitis (DSS3C) and number of tuft cells in the proximal (B) and distal (C) colon. Data presented as mean \pm S.E.M. ($n = 5$ per group) (* $P < 0.05$, ** $P < 0.01$, *** $P < 0.005$. ANOVA followed by the Tukey test).

1022
1023
1024
1025

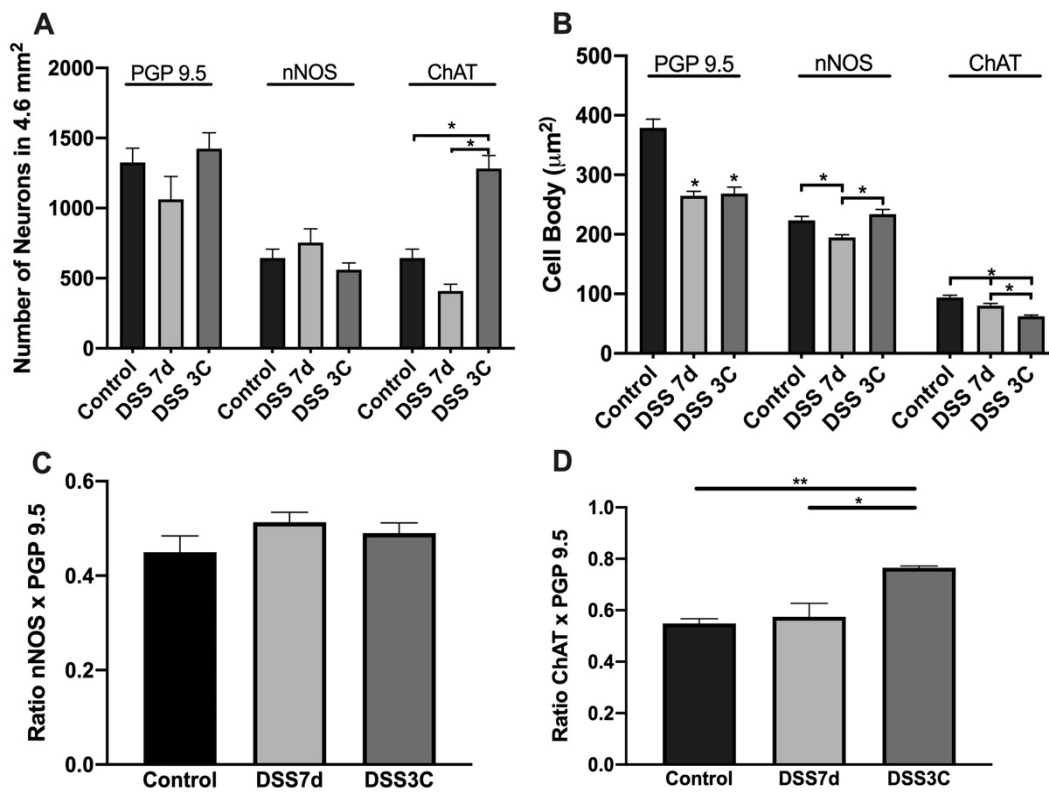


Figure 9 Representative graph of neuronal distribution (**A**) and morphometry (**B**) of neurons of general population (PGP 9.5), nitrenergic (nNOS) and cholinergic (ChAT) positive. (**C**) ChAT x PGP 9.5 ratio and (**D**) nNOS x PGP 9.5 ratio of control mice and exposed to DSS for 7 (DSS7d) days and group with chronic colitis (DSS3C). Data presented as mean \pm S.E.M. (n = 5 per group) (* $P < 0.05$, ** $P < 0.01$, ANOVA followed by the Tukey test).

1026

1027

1028

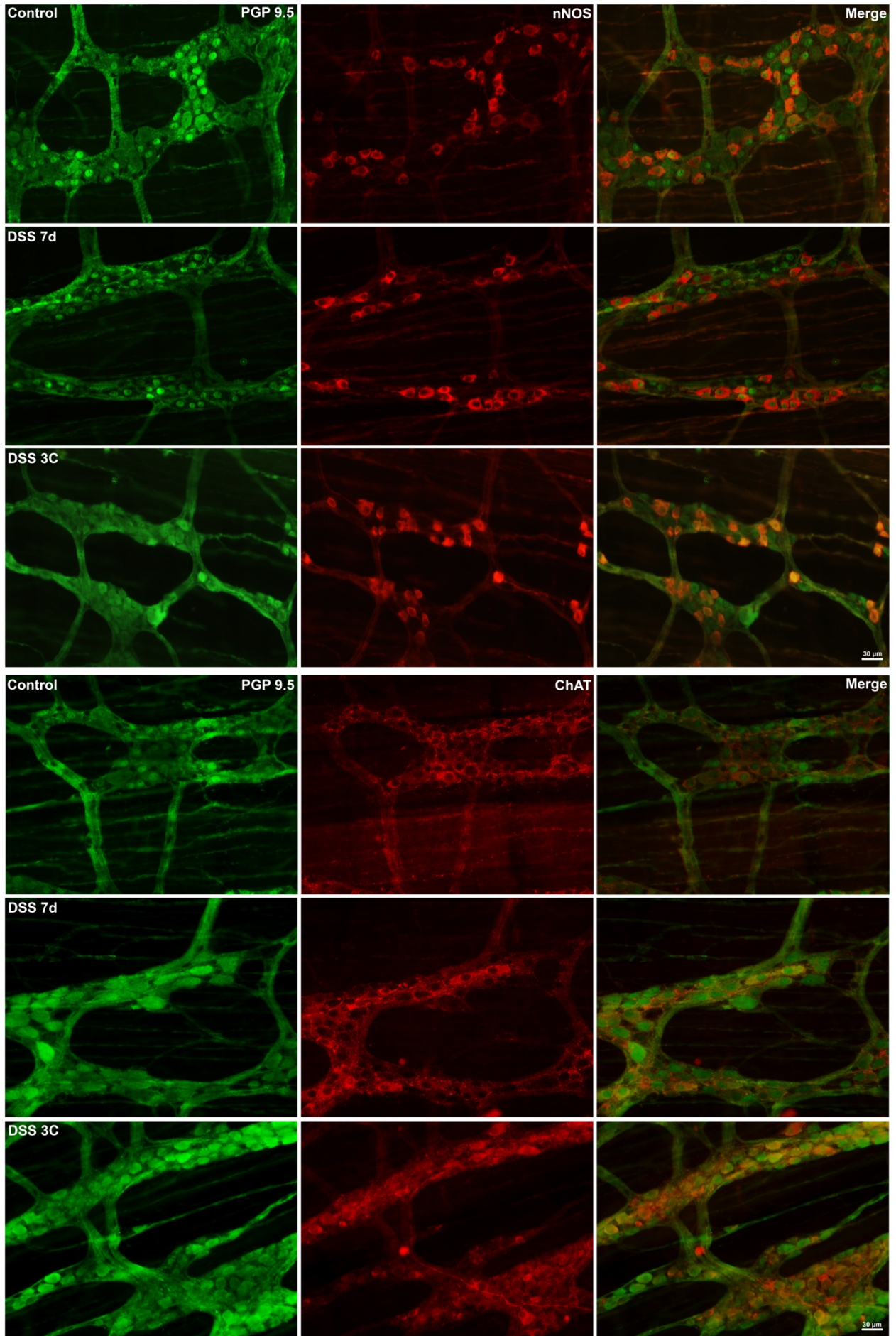


Figure 10 Representative photomicrograph showing the PGP 9.5 +, nNOS + and ChAT + neurons of control group and groups exposed to DSS for 7 days (DSS7d) and chronic colitis (DSS3C).

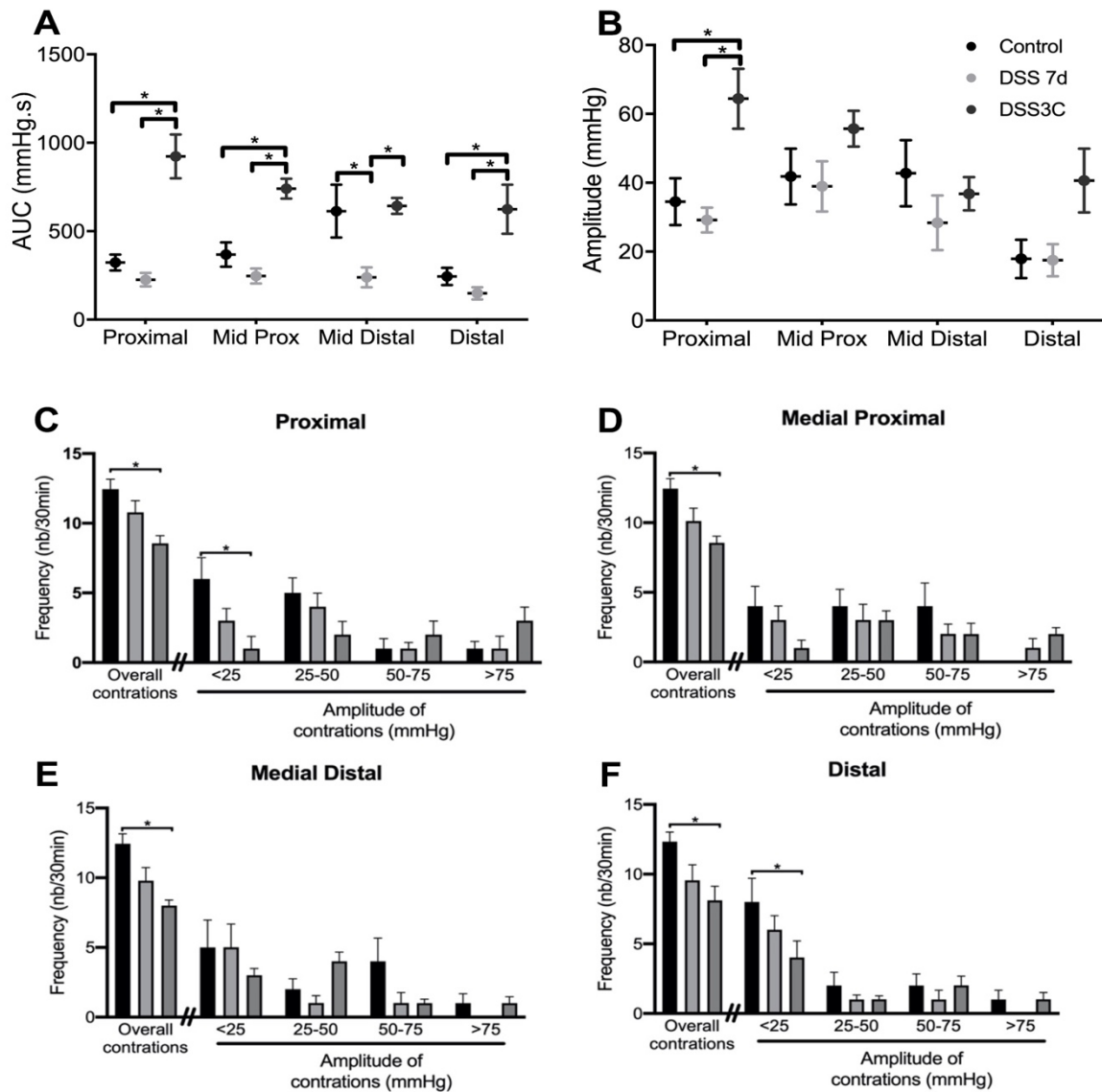


Figure 12 Representative graph of the colonic manometry, comparing control group and groups exposed to the DSS for 7 (DSS7d) days and with chronic colitis (DSS3C). Analyzed parameters: Amplitude of contractions (**A**), area under the curve (AUC) (**B**) and frequency [number (Nb)] that spontaneous contractions occurred, quantified in four categories in the proximal colon (**C**), Proximal Medium (**D**), Medial Distal (**E**) and Distal (**F**). Data presented as mean \pm S.E.M. ($n = 10$ per group) (* $P < 0.05$, ANOVA followed by the Tukey test).

1029

1030

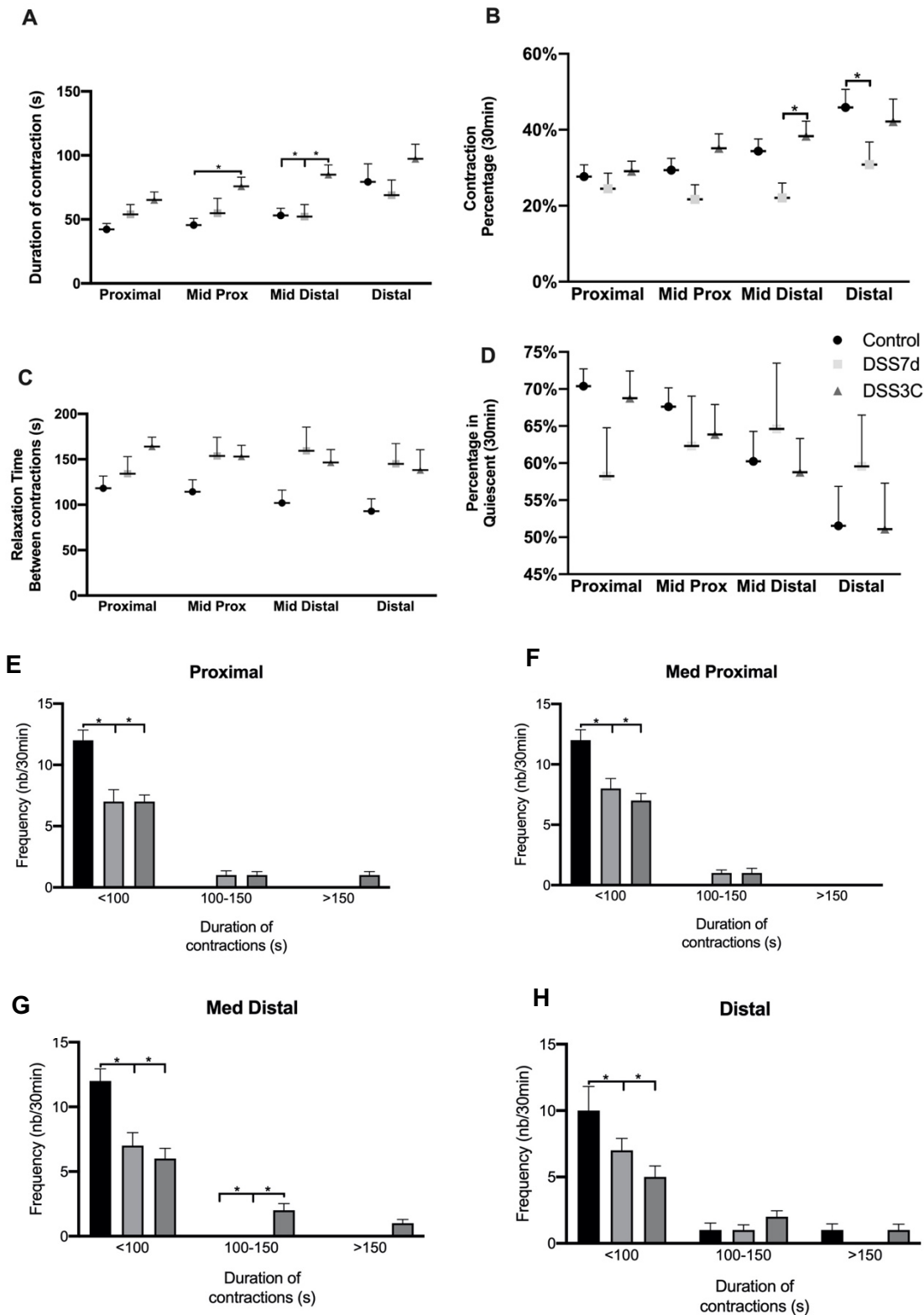


Figure 14 Representative graph of the colonic manometry, comparing control group and groups exposed to the DSS for 7 (DSS7d) days and with chronic colitis (DSS3C). The duration of spontaneous contractions (**A**). The percentage of time the colon remained contracted (**B**). (**C**) the relaxation time between contractions and the percentage of time the colon remained quiescent (**D**) was calculated. The duration of contractions were categorized and quantified [number (Nb) in the proximal (**E**), middle proximal (**F**), distal (**G**) and distal (**H**) colon. Data presented as mean \pm S.E.M. ($n = 10$ per group) (* $P < 0.05$, ANOVA followed by the Tukey test).

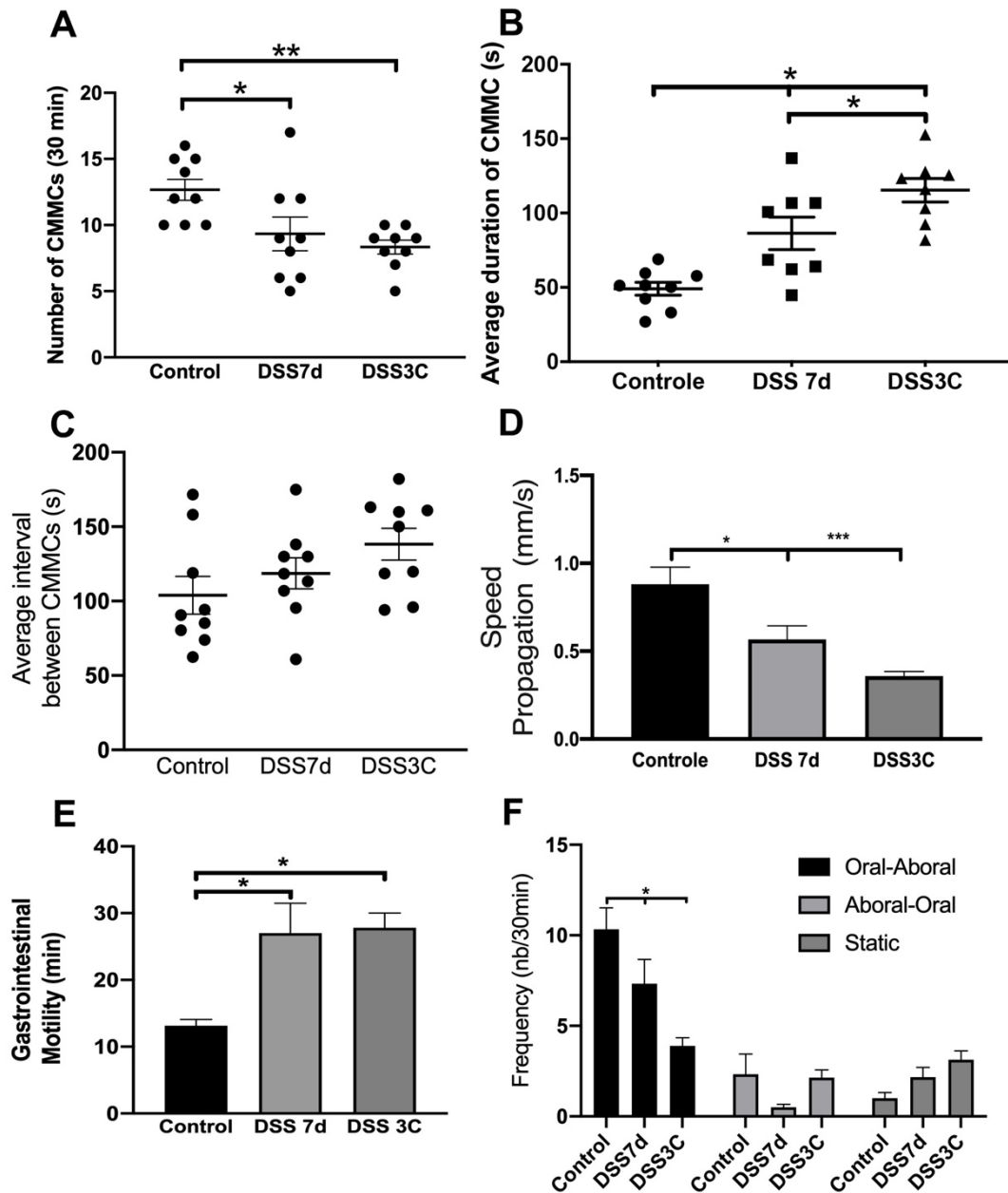


Figure 15 Colonic migratory motor complex (CMMC) profile in mice with acute (DSS7d) and Chronic (DSS3C) colitis. **A:** Plot showing the CMMCs number in 30min. **B:** Average time duration of each CMMC. **C:** Average quiescent time (s) between CMMCs. **D:** Classification of direction and Number (Nb) of CMMCs in 30min. Data presented as mean \pm S.E.M. (n = 10 per group) (* $P < 0.05$; ** $P < 0.01$; *** $P < 0.005$, ANOVA followed by the Tukey test).

1032

1033

1034 4. CONSIDERAÇÕES FINAIS

1035

1036 O uso de DSS foi eficiente para indução química da RCU, tanto no modelo
1037 agudo quanto crônico. A inflamação foi responsável pela diminuição proporcional
1038 no número de células tuft, além de promover alterações histológicas na parede
1039 do cólon e depleção no número de células calciformes e intensa fibrose. Também
1040 foi observado que não ocorre perda neuronal neste modelo, no entanto há uma
1041 mudança no código químico dos neurônios mioentéricos, aumentando os
1042 neurônios ChAT+ nos animais com colite crônica. Todavia os neurônios
1043 mioentéricos estavam atrofiados.

1044 No que tange os estudos de motilidade colônica, encontramos algumas
1045 alterações promovidas pela inflamação como: redução no número de contrações;
1046 aumento na força das contrações, especialmente na porção proximal e distal;
1047 redução no número e aumento na duração dos CMMCs. Sugerimos que essas
1048 alterações no padrão de motilidade fazem parte da adaptação do órgão, sendo
1049 evidente que na colite crônica estas alterações de motilidade são mais intensas.

1050 Diante de todos os resultados aqui obtidos, acreditamos que futuros
1051 experimentos devam ser realizados de modo a entender melhor o papel de outras
1052 células neste modelo de colite induzida por DSS na fase aguda e crônica, como
1053 por exemplo analisar as alterações neuronais no plexo submucoso e
1054 correlacionando com possíveis alterações fisiológicas na secreção do epitélio por
1055 meio da utilização de sistemas de Ussing,

1056 Também seria importante testar alguma estratégia, sendo ela
1057 farmacológica ou biológica, de modo a aumentar a expressão de células tufts
1058 tanto antes quanto depois da indução da colite, estimulando assim uma melhora
1059 da barreira epitelial, amenizando inflamação intestinal, podendo então reduzir os
1060 efeitos deletérios sobre a motilidade colônica. Nesta mesma questão, estudos de
1061 motilidade colônica seriam de extrema importância utilizando fármacos no banho
1062 de órgãos e assim investigar fármacos com potencial de reestabelecer a
1063 motilidade colônica.

1064

1065

1066

- 1067
1068 **5. REFERÊNCIAS**
1069
1070 ABUL ABBAS ANDREW H. LICHTMAN SHIV PILLAI. **Cellular and Molecular**
1071 **Immunology**. 9th. ed. [s.l: s.n.].
1072 ACTIS, G. C.; PELLICANO, R.; FAGOONEE, S.; RIBALDONE, D. G. History of
1073 Inflammatory Bowel Diseases. **Journal of Clinical Medicine**, v. 8, n. 11, p. 1970, 14
1074 nov. 2019.
1075 ALATAB, S.; SEPANLOU, S. G.; IKUTA, K.; VAHEDI, H.; BISIGNANO, C.; SAFIRI,
1076 S.; SADEGHI, A.; NIXON, M. R.; ABDOLI, A.; ABOLHASSANI, H.; ALIPOUR, V.;
1077 ALMADI, M. A. H.; ALMASI-HASHIANI, A.; ANUSHIRAVANI, A.; ARABLOO, J.;
1078 ATIQUE, S.; AWASTHI, A.; BADAWI, A.; BAIG, A. A. A.; et al. The global, regional,
1079 and national burden of inflammatory bowel disease in 195 countries and territories,
1080 1990–2017: a systematic analysis for the Global Burden of Disease Study 2017. **The**
1081 **Lancet Gastroenterology & Hepatology**, v. 5, n. 1, p. 17–30, jan. 2020.
1082 BANERJEE, A.; MCKINLEY, E. T.; VON MOLTKE, J.; COFFEY, R. J.; LAU, K. S.
1083 Interpreting heterogeneity in intestinal tuft cell structure and function. **Journal of**
1084 **Clinical Investigation**, v. 128, n. 5, p. 1711–1719, 1 maio 2018.
1085 BAUMGART, D. C.; SANDBORN, W. J. Inflammatory bowel disease: clinical aspects
1086 and established and evolving therapies. **The Lancet**, v. 369, n. 9573, p. 1641–1657,
1087 maio 2007.
1088 BETTERIDGE, J. D.; ARMBRUSTER, S. P.; MAYDONOVITCH, C.; VEERAPPAN,
1089 G. R. Inflammatory Bowel Disease Prevalence by Age, Gender, Race, and
1090 Geographic Location in the U.S. Military Health Care Population. **Inflammatory**
1091 **Bowel Diseases**, v. 19, n. 7, p. 1421–1427, jun. 2013.
1092 CHASSAING, B.; AITKEN, J. D.; MALLESHAPPA, M.; VIJAY-KUMAR, M. Dextran
1093 Sulfate Sodium (DSS)-Induced Colitis in Mice. **Current Protocols in Immunology**,
1094 v. 104, n. 1, p. 612–615, 4 fev. 2014.
1095 CHILDERS, R. E.; ELURI, S.; VAZQUEZ, C.; WEISE, R. M.; BAYLESS, T. M.;
1096 HUTFLESS, S. Family history of inflammatory bowel disease among patients with
1097 ulcerative colitis: A systematic review and meta-analysis. **Journal of Crohn's and**
1098 **Colitis**, v. 8, n. 11, p. 1480–1497, nov. 2014.
1099 COOPER, H. S.; MURTHY, S. N.; SHAH, R. S.; SEDERGRAN, D. J.
1100 Clinicopathologic study of dextran sulfate sodium experimental murine colitis.
1101 **Laboratory investigation; a journal of technical methods and pathology**, v. 69,

- 1102 n. 2, p. 238–49, ago. 1993.
- 1103 COSKUN, M.; OLSEN, J.; SEIDELIN, J. B.; NIELSEN, O. H. MAP kinases in
1104 inflammatory bowel disease. **Clinica Chimica Acta**, v. 412, n. 7–8, p. 513–520, mar.
1105 2011.
- 1106 COSKUN, M.; SALEM, M.; PEDERSEN, J.; NIELSEN, O. H. Involvement of
1107 JAK/STAT signaling in the pathogenesis of inflammatory bowel disease.
1108 **Pharmacological Research**, v. 76, p. 1–8, out. 2013.
- 1109 COSTA, M.; BROOKES, S. J.; STEELE, P. A.; GIBBINS, I.; BURCHER, E.;
1110 KANDIAH, C. J. Neurochemical classification of myenteric neurons in the guinea-pig
1111 ileum. **Neuroscience**, v. 75, n. 3, p. 949–67, dez. 1996.
- 1112 CURY, D.; OLIVEIRA, R.; CURY, M. Inflammatory bowel diseases: time of
1113 diagnosis, environmental factors, clinical course, and management – a follow-up
1114 study in a private inflammatory bowel disease center (2003–2017). **Journal of**
1115 **Inflammation Research**, v. Volume 12, p. 127–135, maio 2019.
- 1116 DANESE, S.; SANS, M.; FIOCCHI, C. Inflammatory bowel disease: the role of
1117 environmental factors. **Autoimmunity Reviews**, v. 3, n. 5, p. 394–400, jul. 2004.
- 1118 DE GROAT, W. C.; NADELHAFT, I.; MILNE, R. J.; BOOTH, A. M.; MORGAN, C.;
1119 THOR, K. Organization of the sacral parasympathetic reflex pathways to the urinary
1120 bladder and large intestine. **Journal of the Autonomic Nervous System**, v. 3, n. 2–
1121 4, p. 135–160, abr. 1981.
- 1122 DENNING, T. L.; WANG, Y.; PATEL, S. R.; WILLIAMS, I. R.; PULENDRAN, B.
1123 Lamina propria macrophages and dendritic cells differentially induce regulatory and
1124 interleukin 17–producing T cell responses. **Nature Immunology**, v. 8, n. 10, p.
1125 1086–1094, 16 out. 2007.
- 1126 DIGNASS, A.; LINDSAY, J. O.; STURM, A.; WINDSOR, A.; COLOMBEL, J. F.;
1127 ALLEZ, M.; D’HAENS, G.; D’HOORE, A.; MANTZARIS, G.; NOVACEK, G.;
1128 ????RESLAND, T.; REINISCH, W.; SANS, M.; STANGE, E.; VERMEIRE, S.;
1129 TRAVIS, S.; VAN ASSCHE, G. Second European evidence-based consensus on the
1130 diagnosis and management of ulcerative colitis Part 2: Current management.
1131 **Journal of Crohn’s and Colitis**, v. 6, n. 10, p. 991–1030, 2012.
- 1132 DOU, W.; ZHANG, J.; SUN, A.; ZHANG, E.; DING, L.; MUKHERJEE, S.; WEI, X.;
1133 CHOU, G.; WANG, Z.-T.; MANI, S. Protective effect of naringenin against
1134 experimental colitis via suppression of Toll-like receptor 4/NF-κB signalling. **British**
1135 **Journal of Nutrition**, v. 110, n. 4, p. 599–608, 28 ago. 2013.

- 1136 FORD, A. C.; MOAYYEDI, P.; HANAUER, S. B. Ulcerative colitis. **BMJ**, v. 346, n.
1137 feb05 2, p. f432–f432, 5 fev. 2013.
- 1138 FURNESS, J. B. The enteric nervous system and neurogastroenterology. **Nature**
1139 **Reviews Gastroenterology & Hepatology**, v. 9, n. 5, p. 286–294, 6 maio 2012.
- 1140 FURNESS, J.; COSTA, M. **The Enteric Nervous System**. Churchill ed. New York,
1141 NY: [s.n.].
- 1142 FURNESS JB. **The enteric nervous system**. New York: Churchill Livingstone,
1143 2006.
- 1144 GARTNER LP, H. J. **Tratado de Histologia em cores**. Rio de Janeiro: Guanabara
1145 Koogan, 2003.
- 1146 GERBE, F.; JAY, P. Intestinal tuft cells: epithelial sentinels linking luminal cues to the
1147 immune system. **Mucosal Immunology**, v. 9, n. 6, p. 1353–1359, 24 nov. 2016.
- 1148 GERBE, F.; VAN ES, J. H.; MAKRINI, L.; BRULIN, B.; MELLITZER, G.; ROBINE, S.;
1149 ROMAGNOLO, B.; SHROYER, N. F.; BOURGAUX, J.-F.; PIGNODEL, C.;
1150 CLEVERS, H.; JAY, P. Distinct ATOH1 and Neurog3 requirements define tuft cells
1151 as a new secretory cell type in the intestinal epithelium. **The Journal of Cell**
1152 **Biology**, v. 192, n. 5, p. 767–780, 7 mar. 2011.
- 1153 GILAT, T.; HACOHEN, D.; LILOS, P.; LANGMAN, M. J. S. Childhood Factors in
1154 Ulcerative Colitis and Crohn’s Disease: An International Cooperative Study.
1155 **Scandinavian Journal of Gastroenterology**, v. 22, n. 8, p. 1009–1024, 8 jan. 1987.
- 1156 GOYAL, N.; RANA, A.; AHLAWAT, A.; BIJJEM, K. R. V.; KUMAR, P. Animal models
1157 of inflammatory bowel disease: a review. **Inflammopharmacology**, v. 22, n. 4, p.
1158 219–233, 7 ago. 2014.
- 1159 HELLER, F.; FLORIAN, P.; BOJARSKI, C.; RICHTER, J.; CHRIST, M.;
1160 HILLENBRAND, B.; MANKERTZ, J.; GITTER, A.; BURGEL, N.; FROMM, M.
1161 Interleukin-13 Is the Key Effector Th2 Cytokine in Ulcerative Colitis That Affects
1162 Epithelial Tight Junctions, Apoptosis, and Cell Restitution. **Gastroenterology**, v.
1163 129, n. 2, p. 550–564, ago. 2005.
- 1164 HELLER, F.; FROMM, A.; GITTER, A. H.; MANKERTZ, J.; SCHULZKE, J.-D.
1165 Epithelial apoptosis is a prominent feature of the epithelial barrier disturbance in
1166 intestinal inflammation: effect of pro-inflammatory interleukin-13 on epithelial cell
1167 function. **Mucosal Immunology**, v. 1, n. S1, p. S58–S61, 15 nov. 2008.
- 1168 HENDRICKSON, B. A.; GOKHALE, R.; CHO, J. H. Clinical Aspects and
1169 Pathophysiology of Inflammatory Bowel Disease. **Clinical Microbiology Reviews**,

- 1170 v. 15, n. 1, p. 79–94, 1 jan. 2002.
- 1171 HOOVER, B.; BAENA, V.; KAELEBERER, M. M.; GETANEH, F.; CHINCHILLA, S.;
1172 BOHÓRQUEZ, D. V. The intestinal tuft cell nanostructure in 3D. **Scientific Reports**,
1173 v. 7, n. 1, p. 1652, 10 dez. 2017.
- 1174 JOAN, R. O. **A color atlas of the rat : dissection guide**. New York: [s.n].
- 1175 JUNQUEIRA, L.; CARNEIRO, J. **Histologia Básica**. 11. ed. Rio de Janeiro:
1176 Guanabara Koogan, 2008.
- 1177 JUNQUEIRA LC, C. J. **Histologia Básica**. Rio de Janeiro: Guanabara Koogan,
1178 2008.
- 1179 KAPLAN, G. G. The global burden of IBD: from 2015 to 2025. **Nature Reviews**
1180 **Gastroenterology & Hepatology**, v. 12, n. 12, p. 720–727, 1 dez. 2015.
- 1181 KITAJIMA, S.; TAKUMA, S.; MORIMOTO, M. Tissue Distribution of Dextran Sulfate
1182 Sodium(DSS) in the Acute Phase of Murine DSS-Induced Colitis. **Journal of**
1183 **Veterinary Medical Science**, v. 61, n. 1, p. 67–70, 1999.
- 1184 KNIGHTS, D.; LASSEN, K. G.; XAVIER, R. J. Advances in inflammatory bowel
1185 disease pathogenesis: linking host genetics and the microbiome. **Gut**, v. 62, n. 10, p.
1186 1505–1510, out. 2013.
- 1187 LAROUI, H.; INGERSOLL, S. A.; LIU, H. C.; BAKER, M. T.; AYYADURAI, S.;
1188 CHARANIA, M. A.; LAROUI, F.; YAN, Y.; SITARAMAN, S. V.; MERLIN, D. Dextran
1189 Sodium Sulfate (DSS) Induces Colitis in Mice by Forming Nano-Lipocomplexes with
1190 Medium-Chain-Length Fatty Acids in the Colon. **PLoS ONE**, v. 7, n. 3, p. e32084, 9
1191 mar. 2012.
- 1192 LUCIANO, L.; GROOS, S.; REALE, E. Brush Cells of Rodent Gallbladder and
1193 Stomach Epithelia Express Neurofilaments. **Journal of Histochemistry &**
1194 **Cytochemistry**, v. 51, n. 2, p. 187–198, 26 fev. 2003.
- 1195 LYNCH, A. C.; ANTONY, A.; DOBBS, B. R.; FRIZELLE, F. A. Bowel dysfunction
1196 following spinal cord injury. **Spinal Cord**, v. 39, n. 4, p. 193–203, 21 abr. 2001.
- 1197 MALIK, T. A. Inflammatory Bowel Disease. **Surgical Clinics of North America**, v.
1198 95, n. 6, p. 1105–1122, dez. 2015.
- 1199 MATSUDA, N. M.; MILLER, S. M.; EVORA, P. R. B. The chronic gastrointestinal
1200 manifestations of Chagas disease. **Clinics**, v. 64, n. 12, p. 1219–1224, 2009.
- 1201 MELGAR, S.; KARLSSON, A.; MICHAËLSSON, E. Acute colitis induced by dextran
1202 sulfate sodium progresses to chronicity in C57BL/6 but not in BALB/c mice:
1203 correlation between symptoms and inflammation. **American Journal of**

- 1204 **Physiology-Gastrointestinal and Liver Physiology**, v. 288, n. 6, p. G1328–
1205 G1338, jun. 2005.
- 1206 MEYRICK, B.; REID, L. The alveolar brush cell in rat lung—a third pneumonocyte.
1207 **Journal of Ultrastructure Research**, v. 23, n. 1–2, p. 71–80, abr. 1968.
- 1208 MIDDELHOFF, M.; WESTPHALEN, C. B.; HAYAKAWA, Y.; YAN, K. S.; GERSHON,
1209 M. D.; WANG, T. C.; QUANTE, M. Dclk1-expressing tuft cells: Critical modulators of
1210 the intestinal niche? **American Journal of Physiology - Gastrointestinal and**
1211 **Liver Physiology**, v. 313, n. 4, p. G285–G299, 2017.
- 1212 MIR-MADJLESSI, S. H.; MICHENER, W. M.; FARMER, R. G. Course and prognosis
1213 of idiopathic ulcerative proctosigmoiditis in young patients. **Journal of pediatric**
1214 **gastroenterology and nutrition**, v. 5, n. 4, p. 571–5, 1986.
- 1215 MONTELEONE, I.; VAVASSORI, P.; BIANCONE, L.; MONTELEONE, G.;
1216 PALLONE, F. Immunoregulation in the gut: success and failures in human disease.
1217 **Gut**, v. 50, n. Supplement 3, p. iii60–iii64, 1 maio 2002.
- 1218 NAGAO-KITAMOTO, H.; KITAMOTO, S.; KUFFA, P.; KAMADA, N. Pathogenic role
1219 of the gut microbiota in gastrointestinal diseases. **Intestinal Research**, v. 14, n. 2, p.
1220 127, 2016.
- 1221 NIESS, J. H. CX3CR1-Mediated Dendritic Cell Access to the Intestinal Lumen and
1222 Bacterial Clearance. **Science**, v. 307, n. 5707, p. 254–258, 14 jan. 2005.
- 1223 NIKOLAUS, S.; SCHREIBER, S. Diagnostics of Inflammatory Bowel Disease.
1224 **Gastroenterology**, v. 133, n. 5, p. 1670–1689, nov. 2007.
- 1225 OHKUSA, T. [Production of experimental ulcerative colitis in hamsters by dextran
1226 sulfate sodium and changes in intestinal microflora]. **Nihon Shokakibyo Gakkai**
1227 **zasshi = The Japanese journal of gastro-enterology**, v. 82, n. 5, p. 1327–36,
1228 maio 1985.
- 1229 ORDÁS, I.; ECKMANN, L.; TALAMINI, M.; BAUMGART, D. C.; SANDBORN, W. J.
1230 Ulcerative colitis. **The Lancet**, v. 380, n. 9853, p. 1606–1619, nov. 2012.
- 1231 PASTORELLI, L.; DE SALVO, C.; MERCADO, J. R.; VECCHI, M.; PIZARRO, T. T.
1232 Central Role of the Gut Epithelial Barrier in the Pathogenesis of Chronic Intestinal
1233 Inflammation: Lessons Learned from Animal Models and Human Genetics.
1234 **Frontiers in Immunology**, v. 4, 2013.
- 1235 PEDERSEN, J. Inflammatory pathways of importance for management of
1236 inflammatory bowel disease. **World Journal of Gastroenterology**, v. 20, n. 1, p. 64,
1237 2014.

- 1238 PERŠE, M.; CERAR, A. Dextran Sodium Sulphate Colitis Mouse Model: Traps and
1239 Tricks. **Journal of Biomedicine and Biotechnology**, v. 2012, p. 1–13, 2012.
- 1240 ROGERS, B. H. G.; CLARK, L. M.; KIRSNER, J. B. The epidemiologic and
1241 demographic characteristics of inflammatory bowel disease: An analysis of a
1242 computerized file of 1400 patients. **Journal of Chronic Diseases**, v. 24, n. 12, p.
1243 743–773, dez. 1971.
- 1244 RUHL, A.; NASSER, Y.; SHARKEY, K. A. Enteric glia. **Neurogastroenterology and**
1245 **Motility**, v. 16, n. s1, p. 44–49, abr. 2004.
- 1246 SANT’ANA, D.; MIRANDA-NETO, M.; OLIVEIRA, L. **Anatomia Humana:**
1247 **Apendizagem Dinâmica**. Maringá-PR: [s.n.].
- 1248 SIEGMUND, B.; ZEITZ, M. Innate and adaptive immunity in inflammatory bowel
1249 disease. **World journal of gastroenterology**, v. 17, n. 27, p. 3178–83, 21 jul. 2011.
- 1250 SMITH, T. K.; SPENCER, N. J.; HENNIG, G. W.; DICKSON, E. J. Recent
1251 advances in enteric neurobiology: mechanosensitive interneurons.
1252 **Neurogastroenterology & Motility**, v. 19, n. 11, p. 869–878, nov. 2007.
- 1253 SMYTHIES, L. E.; SHEN, R.; BIMCZOK, D.; NOVAK, L.; CLEMENTS, R. H.;
1254 ECKHOFF, D. E.; BOUCHARD, P.; GEORGE, M. D.; HU, W. K.; DANDEKAR, S.;
1255 SMITH, P. D. Inflammation Anergy in Human Intestinal Macrophages Is Due to
1256 Smad-induced I κ B α Expression and NF- κ B Inactivation. **Journal of Biological**
1257 **Chemistry**, v. 285, n. 25, p. 19593–19604, 18 jun. 2010.
- 1258 SPEHLMANN, M. E.; BEGUN, A. Z.; BURGHARDT, J.; LEPAGE, P.; RAEDLER, A.;
1259 SCHREIBER, S. Epidemiology of inflammatory bowel disease in a German twin
1260 cohort: Results of a nationwide study. **Inflammatory Bowel Diseases**, v. 14, n. 7, p.
1261 968–976, jul. 2008.
- 1262 SPENCER, N. J.; DINNING, P. G.; BROOKES, S. J.; COSTA, M. Insights into the
1263 mechanisms underlying colonic motor patterns. **The Journal of Physiology**, v. 594,
1264 n. 15, p. 4099–4116, 1 ago. 2016.
- 1265 SWENSON, O. Hirschsprung’s Disease: A Review. **PEDIATRICS**, v. 109, n. 5, p.
1266 914–918, 1 maio 2002.
- 1267 SWIRSKI, F. K.; NAHRENDORF, M.; ETZRODT, M.; WILDGRUBER, M.; CORTEZ-
1268 RETAMOZO, V.; PANIZZI, P.; FIGUEIREDO, J.-L.; KOHLER, R. H.;
1269 CHUDNOVSKIY, A.; WATERMAN, P.; AIKAWA, E.; MEMPEL, T. R.; LIBBY, P.;
1270 WEISSLEDER, R.; PITTET, M. J. Identification of splenic reservoir monocytes and
1271 their deployment to inflammatory sites. **Science (New York, N.Y.)**, v. 325, n. 5940,

- 1272 p. 612–6, 31 jul. 2009.
- 1273 VAN ASSCHE, G.; DIGNASS, A.; PANES, J.; BEAUGERIE, L.; KARAGIANNIS, J.;
- 1274 ALLEZ, M.; OCHSENKÜHN, T.; ORCHARD, T.; ROGLER, G.; LOUIS, E.;
- 1275 KUPCINSKAS, L.; MANTZARIS, G.; TRAVIS, S.; STANGE, E. The second
- 1276 European evidence-based Consensus on the diagnosis and management of Crohn's
- 1277 disease: Definitions and diagnosis. **Journal of Crohn's and Colitis**, v. 4, n. 1, p. 7–
- 1278 27, 1 fev. 2010.
- 1279 VAUGHN, B. P.; MOSS, A. C. Novel treatment options for ulcerative colitis. **Clinical**
- 1280 **Investigation**, v. 3, n. 11, p. 1057–1069, nov. 2013.
- 1281 VERMEIRE, S.; RUTGEERTS, P. Pathogenesis and management of IBD—thinking
- 1282 outside the box. **Nature Reviews Gastroenterology & Hepatology**, v. 10, n. 2, p.
- 1283 67–69, 8 fev. 2013.
- 1284 VICTORIA, C. R.; SASSAK, L. Y.; NUNES, H. R. DE C. Incidence and prevalence
- 1285 rates of inflammatory bowel diseases, in midwestern of São Paulo State, Brazil.
- 1286 **Arquivos de Gastroenterologia**, v. 46, n. 1, p. 20–25, mar. 2009.
- 1287 VON MOLTKE, J.; JI, M.; LIANG, H.-E.; LOCKSLEY, R. M. Tuft-cell-derived IL-25
- 1288 regulates an intestinal ILC2–epithelial response circuit. **Nature**, v. 529, n. 7585, p.
- 1289 221–225, 14 jan. 2016.
- 1290 WALLACE, K. L. Immunopathology of inflammatory bowel disease. **World Journal**
- 1291 **of Gastroenterology**, v. 20, n. 1, p. 6, 2014.
- 1292 WU, W.; CHEN, F.; LIU, Z.; CONG, Y. Microbiota-specific Th17 Cells. **Inflammatory**
- 1293 **Bowel Diseases**, v. 22, n. 6, p. 1473–1482, jun. 2016.
- 1294 ZHANG, Y.-Z. Inflammatory bowel disease: Pathogenesis. **World Journal of**
- 1295 **Gastroenterology**, v. 20, n. 1, p. 91, 2014.
- 1296
- 1297
- 1298

1299
1300
1301
1302
1303
1304
1305
1306
1307
1308
1309
1310
1311
1312
1313
1314
1315

ANEXOS

- 1316 **A**
 1317 Aprovação da Comissão de Ética no Uso de Animais da Universidade Estadual de
 1318 Londrina (CEUA/UUEL) processo 4023.2017.31.



UNIVERSIDADE
ESTADUAL DE LONDRINA

COMISSÃO DE ÉTICA NO USO DE ANIMAIS

OF. CIRC. CEUA Nº 48/2017

Londrina, 05 Maio de 2017.

Prezado Profº.

Certificamos que o projeto intitulado: "**Efeitos da fototerapia durante a colite experimental crônica induzida por sulfato sódico de dextrana (DSS) em camundongos**" protocolo CEUA nº**4023.2017.31**, sob a responsabilidade de **Eduardo José de Almeida Araujo**, que envolve a produção, manutenção e/ou utilização de animais pertencentes ao filo Chordata, subfilo Vertebrata (exceto o homem) para fins de pesquisa científica (ou ensino), encontra-se de acordo com os preceitos da Lei nº 11.794, de 8 de outubro de 2008, do Decreto nº 6.899, de 15 de julho de 2009, e com as normas editadas pelo Conselho Nacional de Controle da Experimentação Animal (CONCEA), foi **aprovado** pela Comissão de Ética no Uso de Animais da Universidade Estadual de Londrina (CEUA/UUEL), em reunião realizada em **02/05/2017**

O Objetivo do projeto é avaliar o potencial anti-inflamatório da luz com comprimento de onda na faixa do infravermelho (próximo a 940 nm) sobre a colite crônica induzida pela administração do DSS em camundongos. Grau de invasividade =2

Vigência do Projeto	01/06/2017 a 28/02/2020
Espécie/linhagem	Camundongos Isogênico (C57Bl/6)
Nº de animais	156
Peso/Idade	20-25 g / 2 meses
Sexo	Machos
Origem	Biotério da UEL/ CCB
Amostras a serem coletadas	Cólon

Cumpra orientar que caso pretendam-se quaisquer alterações no protocolo experimental aprovado, deve-se submeter o novo protocolo à apreciação da CEUA/UUEL anteriormente à execução das modificações.

Coloco-me à disposição para quaisquer esclarecimentos que se fizerem necessária. Sem mais para o momento, subscrevo, cordialmente,

Prof.ª Dra. Glaucia Scantamburlo Alves Fernandes
 Coordenadora da CEUA/UUEL

Ilmo. Sr.
Prof. Dr. Eduardo José de Almeida Araujo
 Responsável pelo projeto
 Departamento de Histologia/CCB.

1320

1321 **B - Normas da revista *Neurogastroenterology and motility* (fator de impactor**
 1322 **2.946)**

1323

1324 **PREPARING YOUR SUBMISSION**

1325 **Cover Letters**

1326 A covering letter must be included, signed by the corresponding author and stating on
 1327 behalf of all the authors that the work has not been published and is not being considered
 1328 for publication elsewhere.

1329 **Parts of the Manuscript**

1330 The manuscript should be submitted in separate files: main text file; figures.

1331 The manuscript should be double-spaced with 30mm margins. Manuscripts must be
 1332 numbered consecutively in the following sequence: Title Page; Abstract, if required; Main
 1333 Body of Text; Acknowledgement; Reference List; Tables and Figure caption List.

- 1334 i. A short informative title containing the major key words. The title should not contain
 1335 abbreviations (see Wiley's [Wiley's best practice SEO tips](#));
- 1336 ii. A short running title of less than 40 characters;
- 1337 iii. The full names of the authors;
- 1338 iv. The author's institutional affiliations where the work was conducted, with a footnote
 1339 for the author's present address if different from where the work was conducted;
- 1340 v. Acknowledgments;
- 1341 vi. Abstract and keywords;
- 1342 vii. Graphical Abstract;
- 1343 viii. Main text;
- 1344 ix. References;
- 1345 x. Tables (each table complete with title and footnotes);
- 1346 xi. Figure legends;
- 1347 xii. Appendices (if relevant).

1348 Figures and supporting information should be supplied as separate files.

1349 **Title page**

1350 On the title page, provide the complete title and a running title (not to exceed 45 characters
 1351 and spaces). List each contributor's name and institutional affiliation. Provide the name,
 1352 postal and e-mail address, fax and telephone number of the contributor responsible for the
 1353 manuscript and proofs. This is the person to whom all correspondence will be sent. The
 1354 corresponding author is responsible for keeping the editorial office updated with any
 1355 change in details until the paper is published.

1356 **Authorship**

1357 Please refer to the journal's Authorship policy in the Editorial Policies and Ethical
 1358 Considerations section for details on author listing eligibility.

1359 **Acknowledgments**

1360 Contributions from anyone who does not meet the criteria for authorship should be listed,
 1361 with permission from the contributor, in an Acknowledgments section. Financial and

1362 material support should also be mentioned. Thanks to anonymous reviewers are not
1363 appropriate.

1364 **Conflict of Interest Statement**

1365 Authors will be asked to provide a conflict of interest statement during the submission
1366 process. For details on what to include in this section, see the 'Conflict of Interest' section in
1367 the Editorial Policies and Ethical Considerations section below. Submitting authors should
1368 ensure they liaise with all co-authors to confirm agreement with the final statement.

1369

1370 **Abstract and Keywords**

1371 The abstract must not exceed 250 words. It should summarize the aim of the study and
1372 describe the work undertaken, results and conclusions. For Original Articles and Technical
1373 Notes, the abstract should be structured under four subheadings: **Background, Methods,**
1374 **Key Results and Conclusions & Inferences.** For Review Articles, the abstract should be
1375 structured under **Background and Purpose.** For Mini-review editorials, "Hot Topics" and
1376 Case Reports, the abstract should be unstructured, i.e. without the subheadings. In addition,
1377 you should list up to six keywords in alphabetical order. For ideas on optimising your
1378 abstract, see [here](#).

1379

1380 **Keywords**

1381 Please provide 5-7 keywords. Keywords should be taken from those recommended by the
1382 US National Library of Medicine's Medical Subject Headings (MeSH) browser list
1383 at <https://www.nlm.nih.gov/mesh/>.

1384 **Main body of text**

1385 Manuscripts should be typed in a standard, easy to read font, either 11 or 12pt in size.
1386 Manuscripts should be double-spaced, with 2.5cm (1 inch) margins on all sides and run in
1387 one single column. Please ensure that you have turned "track changes off" and removed any
1388 reviewing notes from your manuscripts else these will be visible throughout the review
1389 process. Place the page number and first author's last name in the upper right-hand corner
1390 of each page.

1391 Review articles should be divided onto the following sections and appear in the following
1392 order: (1) title page (with short running page heading, title, authors names and affiliations),
1393 (2) abstract and keywords, (3) body of the article, (4) acknowledgments, funding, and
1394 disclosures; (5) references, (6) tables, (7) figure legends, and (8) figures.

1395 Original articles should be divided into the following sections and appear in the following
1396 order: (1) title page (with short running page heading, title, authors names and affiliations)
1397 (2) abstract and keywords, (3) introduction, (4) materials and methods, (5) results, (6)
1398 discussion, (7) acknowledgments, funding, and disclosures, (8) references, (9) appendices,
1399 (10) supporting information, (11) tables, (12) figure legends, and (13) figures.

1400 **Methods and Materials**

1401 Animal preparation and experimentation should cite the approving governing body.
1402 Equipment and apparatus should cite the make and model number and the company name
1403 and address (town, state/city, country) at first mention.

1404 Give all measurements in metric units and use negative indexing (mg mL⁻¹, not mg/mL). Use
1405 generic names of drugs. Symbols, units and abbreviations should be expressed as Système
1406 International (SI) units. In exceptional circumstances, others may be used, provided they are
1407 consistent. If necessary, please contact the editorial office for further advice.

1408 **[Experimental Methods Reporting Checklist for Authors](#)**

1409 **References**

1410 All references should be numbered consecutively in order of appearance and should be as
1411 complete as possible. In text citations should cite references in consecutive order using
1412 Arabic superscript numerals. Sample references follow:

1413 Journal article:

1414 1. King VM, Armstrong DM, Apps R, Trott JR. Numerical aspects of pontine, lateral reticular,
1415 and inferior olivary projections to two paravermal cortical zones of the cat cerebellum. *J*
1416 *Comp Neurol* 1998;390:537-551.

1417 Book:

1418 2. Voet D, Voet JG. Biochemistry. New York: John Wiley & Sons; 1990. 1223 p.

1419 Please note that journal title abbreviations should conform to the practices of Chemical
1420 Abstracts.

1421 For more information about AMA reference style - **[AMA Manual of Style](#)**.

1422 **Endnotes**

1423 Endnotes should be placed as a list at the end of the paper only, not at the foot of each
1424 page. They should be numbered in the list and referred to in the text with consecutive,
1425 superscript Arabic numerals. Keep endnotes brief; they should contain only short
1426 comments tangential to the main argument of the paper.

1427 **Footnotes**

1428 Footnotes should be placed as a list at the end of the paper only, not at the foot of each
1429 page. They should be numbered in the list and referred to in the text with consecutive,
1430 superscript Arabic numerals. Keep footnotes brief; they should contain only short
1431 comments tangential to the main argument of the paper and should not include references.

1432 **Tables**

1433 Tables should be self-contained and complement, not duplicate, information contained in
1434 the text. They should be supplied as editable files, not pasted as images. Legends should be
1435 concise but comprehensive – the table, legend, and footnotes must be understandable
1436 without reference to the text. All abbreviations must be defined in footnotes. Footnote
1437 symbols: †, ‡, §, ¶, should be used (in that order) and *, **, *** should be reserved for P-
1438 values. Statistical measures such as SD or SEM should be identified in the headings.

1439 **Figure Legends**

1440 Legends should be concise but comprehensive – the figure and its legend must be
1441 understandable without reference to the text. Include definitions of any symbols used and
1442 define/explain all abbreviations and units of measurement.

1443 **Figures**

1444 Although authors are encouraged to send the highest-quality figures possible, for peer-
1445 review purposes, a wide variety of formats, sizes, and resolutions are accepted.

1446 **[Click here](#)** for the basic figure requirements for figures submitted with manuscripts for
1447 initial peer review, as well as the more detailed post-acceptance figure requirements.

1448 **Color figures.** Figures submitted in colour may be reproduced in colour online free of
1449 charge. Please note, however, that it is preferable that line figures (e.g. graphs and charts)
1450 are supplied in black and white so that they are legible if printed by a reader in black and
1451 white.

1452 **Data Citation**

1453 In recognition of the significance of data as an output of research effort, Wiley has endorsed
 1454 In recognition of the significance of data as an output of research effort, Wiley has endorsed
 1455 the [FORCE11 Data Citation Principles](#) and is implementing a mandatory data citation
 1456 policy. Wiley journals require data to be cited in the same way as article, book, and web
 1457 citations and authors are required to include data citations as part of their reference list.

1458 Data citation is appropriate for data held within institutional, subject focused, or more
 1459 general data repositories. It is not intended to take the place of community standards such
 1460 as in-line citation of GenBank accession codes.

1461 When citing or making claims based on data, authors must refer to the data at the relevant
 1462 place in the manuscript text and in addition provide a formal citation in the reference list.

1463 We recommend the format proposed by the [Joint Declaration of Data Citation Principles](#):

- 1464 • [dataset] Authors; Year; Dataset title; Data repository or archive; Version (if any);
 1465 Persistent identifier (e.g. DOI)

1466 **Additional Files**

1467 **Appendices**

1468 Appendices will be published after the references. For submission they should be supplied
 1469 as separate files but referred to in the text.

1470 **Supporting Information**

1471 Supporting information is information that is not essential to the article but provides
 1472 greater depth and background. It is hosted online and appears without editing or
 1473 typesetting. It may include tables, figures, videos, datasets, etc.

1474 [Click here](#) for Wiley's FAQs on supporting information.

1475 Note: if data, scripts, or other artefacts used to generate the analyses presented in the
 1476 paper are available via a publicly available data repository, authors should include a
 1477 reference to the location of the material within their paper.

1478 **General Style Points**

1479 The following points provide general advice on formatting and style.

- 1480 • Abbreviations: In general, terms should not be abbreviated unless they are used
 1481 repeatedly, and the abbreviation is helpful to the reader. Initially, use the word in
 1482 full, followed by the abbreviation in parentheses. Thereafter use the abbreviation
 1483 only.
- 1484 • Units of measurement: Measurements should be given in SI or SI-derived units. Visit
 1485 the Bureau International des Poids et Mesures (BIPM) website for more information
 1486 about SI units.
- 1487 • Numbers: numbers under 10 are spelt out, except for: measurements with a unit
 1488 (8mmol/l); age (6 weeks old), or lists with other numbers (11 dogs, 9 cats, 4 gerbils).
- 1489 • Trade Names: Chemical substances should be referred to by the generic name only.
 1490 Trade names should not be used. Drugs should be referred to by their generic
 1491 names. If proprietary drugs have been used in the study, refer to these by their
 1492 generic name, mentioning the proprietary name and the name and location of the
 1493 manufacturer in parentheses.

1494 **Wiley Author Resources**

1495 **Manuscript Preparation Tips:** Wiley has a range of resources for authors preparing
 1496 manuscripts for submission available [here](#). In particular, we encourage authors to consult
 1497 Wiley's best practice tips on [Writing for Search Engine Optimization](#).

1498 **Article Preparation Support**

1499 [Wiley Editing Services](#) offers expert help with English Language Editing, as well as translation,
 1500 manuscript formatting, figure illustration, figure formatting, and graphical abstract design – so
 1501 you can submit your manuscript with confidence.

1502 Also, check out our resources for [Preparing Your Article](#) for general guidance about writing and
 1503 preparing your manuscript.

1504

1505 **5. EDITORIAL POLICIES AND ETHICAL CONSIDERATIONS**

1506 **Peer Review and Acceptance**

1507 The acceptance criteria for all papers are the quality and originality of the research and its
 1508 significance to our readership. Papers will only be sent to review if the Editor-in-Chief
 1509 determine that the paper meets the appropriate quality and relevance requirements.

1510 Wiley's policy on confidentiality of the review process is available [here](#).

1511 **Guidelines on Publishing and Research Ethics in Journal Articles** Please review Wiley's
 1512 policies surrounding human studies, animal studies, clinical trial registration, biosecurity,
 1513 and research reporting guidelines [here](#).

1514 **Species Names**

1515 Upon its first use in the title, abstract, and text, the common name of a species should be
 1516 followed by the scientific name (genus, species, and authority) in parentheses. For well-
 1517 known species, however, scientific names may be omitted from article titles. If no common
 1518 name exists in English, only the scientific name should be used.

1519 **Genetic Nomenclature**

1520 Sequence variants should be described in the text and tables using both DNA and protein
 1521 designations whenever appropriate. Sequence variant nomenclature must follow the
 1522 current HGVS guidelines; see <http://varnomen.hgvs.org/>, where examples of acceptable
 1523 nomenclature are provided.

1524 **Nucleotide sequence data** can be submitted in electronic form to any of the three major
 1525 collaborative databases: DDBJ, EMBL, or GenBank. It is only necessary to submit to one
 1526 database as data are exchanged between DDBJ, EMBL, and GenBank on a daily basis. The
 1527 suggested wording for referring to accession-number information is: 'These sequence data
 1528 have been submitted to the DDBJ/EMBL/GenBank databases under accession number
 1529 U12345'. Addresses are as follows:

- 1530 • DNA Data Bank of Japan (DDBJ) www.ddbj.nig.ac.jp
- 1531 • EMBL Nucleotide Archive: ebi.ac.uk/ena
- 1532 • GenBank www.ncbi.nlm.nih.gov/genbank

1533 **Proteins sequence data** should be submitted to either of the following repositories:

- 1534 • Protein Information Resource (PIR): pir.georgetown.edu
- 1535 • SWISS-PROT: expasy.ch/sprot/sprot-top

1536 **Conflict of Interest**

1537 The journal requires that all authors disclose any potential sources of conflict of interest.
 1538 Any interest or relationship, financial or otherwise that might be perceived as influencing an
 1539 author's objectivity is considered a potential source of conflict of interest. These must be
 1540 disclosed when directly relevant or directly related to the work that the authors describe in
 1541 their manuscript. Potential sources of conflict of interest include, but are not limited to,
 1542 patent or stock ownership, membership of a company board of directors, membership of
 1543 an advisory board or committee for a company, and consultancy for or receipt of speaker's
 1544 fees from a company. The existence of a conflict of interest does not preclude publication. If
 1545 the authors have no conflict of interest to declare, they must also state this at submission. It
 1546 is the responsibility of the corresponding author to review this policy with all authors and
 1547 collectively to disclose with the submission ALL pertinent commercial and other
 1548 relationships.

1549 **Funding**

1550 Authors should list all funding sources in the Acknowledgments section. Authors are
 1551 responsible for the accuracy of their funder designation. If in doubt, please check the Open
 1552 Funder Registry for the correct
 1553 nomenclature: <http://www.crossref.org/fundingdata/registry.html>

1554 **Authorship**

1555 The journal follows the [ICMJE definition of authorship](#), which indicates that authorship be
 1556 based on the following 4 criteria:

- 1557 • Substantial contributions to the conception or design of the work; or the acquisition,
 1558 analysis, or interpretation of data for the work; AND
- 1559 • Drafting the work or revising it critically for important intellectual content; AND
- 1560 • Final approval of the version to be published; AND
- 1561 • Agreement to be accountable for all aspects of the work in ensuring that questions
 1562 related to the accuracy or integrity of any part of the work are appropriately
 1563 investigated and resolved.

1564 In addition to being accountable for the parts of the work he or she has done, an author
 1565 should be able to identify which co-authors are responsible for specific other parts of the
 1566 work. In addition, authors should have confidence in the integrity of the contributions of
 1567 their co-authors.

1568 All those designated as authors should meet all four criteria for authorship, and all who
 1569 meet the four criteria should be identified as authors. Those who do not meet all four
 1570 criteria should be acknowledged. These authorship criteria are intended to reserve the
 1571 status of authorship for those who deserve credit and can take responsibility for the work.
 1572 The criteria are not intended for use as a means to disqualify colleagues from authorship
 1573 who otherwise meet authorship criteria by denying them the opportunity to meet criterion
 1574 #s 2 or 3. Therefore, all individuals who meet the first criterion should have the opportunity
 1575 to participate in the review, drafting, and final approval of the manuscript.

1576 **Data Sharing and Data Accessibility**

1577 The journal encourages authors to share the data and other artefacts supporting the results
 1578 in the paper by archiving it in an appropriate public repository. Authors should include a
 1579 data accessibility statement, including a link to the repository they have used, in order that
 1580 this statement can be published alongside their paper.

1581 **Data Citation**

1582 Please also cite the data you have shared, like you would cite other sources that your article
 1583 refers to, in your references section. You should follow the format for your data citations
 1584 laid out in the Joint Declaration of Data Citation
 1585 Principles, <https://www.force11.org/datacitationprinciples>:

- 1586 • [dataset] Authors; Year; Dataset title; Data repository or archive; Version (if any);
 1587 Persistent identifier (e.g. DOI)

1588 **Human subject information in databases.** The journal refers to the [World Health
 1589 Medical Association Declaration of Taipei on Ethical Considerations Regarding Health
 1590 Databases and Biobanks](#).

1591 **Publication Ethics**

1592 This journal is a member of the [Committee on Publication Ethics \(COPE\)](#). Note this journal
 1593 uses iThenticate's CrossCheck software to detect instances of overlapping and similar text in
 1594 submitted manuscripts. Read Wiley's Top 10 Publishing Ethics Tips for Authors [here](#). Wiley's
 1595 Publication Ethics Guidelines can be found [here](#).

1596 **ORCID**

1597 As part of our commitment to supporting authors at every step of the publishing
 1598 process, *Cytopathology* requires the submitting author (only) to provide an ORCID iD when
 1599 submitting a manuscript. This takes around 2 minutes to complete. [Find more
 1600 information](#).

1601 **6. AUTHOR LICENSING**

1602 If your paper is accepted, the author identified as the formal corresponding author will
 1603 receive an email prompting them to log in to Author Services, where via the Wiley Author
 1604 Licensing Service (WALS) they will be required to complete a copyright license agreement on
 1605 behalf of all authors of the paper.

1606 Authors may choose to publish under the terms of the journal's standard copyright
 1607 agreement, or [OnlineOpen](#) under the terms of a Creative Commons License.

1608 General information regarding licensing and copyright is available [here](#). To review the
 1609 Creative Commons License options offered under OnlineOpen, please [click here](#). (Note that
 1610 certain funders mandate that a particular type of CC license has to be used; to check this
 1611 please [click here](#).)

1612 **Self-Archiving definitions and policies.** Note that the journal's standard copyright
 1613 agreement allows for self-archiving of different versions of the article under specific
 1614 conditions. Please click [here](#) for more detailed information about self-archiving definitions
 1615 and policies.

1616 **Open Access fees:** If you choose to publish using OnlineOpen you will be charged a fee. A list
 1617 of Article Publication Charges for Wiley journals is available [here](#).

1618 **Funder Open Access:** Please click [here](#) for more information on Wiley's compliance with
 1619 specific Funder Open Access Policies.

1620 **7. PUBLICATION PROCESS AFTER ACCEPTANCE**

1621 **Accepted article received in production**

1622 When your accepted article is received by Wiley's production team, you (corresponding

1623 author) will receive an email asking you to login or register with [Author Services](#). You will
1624 be asked to sign a publication license at this point.